



Royal Netherlands Institute for Sea Research

This is a preprint of:

Villanueva, L., Schouten, S. & Sinninghe Damsté, J.S. (2016). Phylogenomic analysis of lipid biosynthetic genes of Archaea shed light on the 'lipid divide'. *Environmental Microbiology*, 19(1), 54-69.

Published version: dx.doi.org/10.1111/1462-2920.13361

Link NIOZ Repository: www.vliz.be/nl/imis?module=ref&refid=259343

[Article begins on next page]

The NIOZ Repository gives free access to the digital collection of the work of the Royal Netherlands Institute for Sea Research. This archive is managed according to the principles of the [Open Access Movement](#), and the [Open Archive Initiative](#). Each publication should be cited to its original source - please use the reference as presented.

When using parts of, or whole publications in your own work, permission from the author(s) or copyright holder(s) is always needed.

Phylogenomic analysis of lipid biosynthetic genes of Archaea shed light on the ‘lipid divide’

Laura Villanueva^{1*}, Stefan Schouten^{1,2}, and Jaap S. Sinninghe Damsté^{1,2}

¹NIOZ, Royal Netherlands Institute for Sea Research. Department of Marine Microbiology and Biogeochemistry, and Utrecht University, P.O. Box 59, NL-1790 AB Den Burg, Texel, The Netherlands.

²Utrecht University, Faculty of Geosciences, P.O. Box 80.021, 3508 TA Utrecht, The Netherlands

*Correspondence to L.V. e-mail: laura.villanueva@nioz.nl

Resubmitted to Environmental Microbiology

Running title: Archaeal lipid biosynthesis and the lipid divide

Keywords: ‘lipid divide’, Archaea, membrane lipids, glycerol stereochemistry, fatty acid synthesis, Lokiarchaeum, uncultured marine euryarchaeota group II and III.

1 **Summary**

2 The lipid membrane is one of the most characteristic traits distinguishing the three domains of
3 life. Membrane lipids of Bacteria and Eukarya are composed of fatty acids linked to glycerol-3-
4 phosphate (G3P) via ester bonds, while those of Archaea possess isoprene-based alkyl chains linked
5 by ether linkages to glycerol-1-phosphate (G1P), resulting in the opposite stereochemistry of the
6 glycerol phosphate backbone. This 'lipid divide' has raised questions on the evolution of microbial
7 life since eukaryotes are thought to have evolved from the Archaea, requiring a radical change in
8 membrane composition. Here, we searched for homologs of enzymes involved in membrane lipid
9 and fatty acid synthesis in a wide variety of archaeal genomes and performed phylogenomic
10 analyses. We found that two uncultured archaeal groups, i.e. marine euryarchaeota group II/III and
11 'Lokiarchaeota', recently discovered descendants of the archaeal ancestor leading to eukaryotes,
12 lack the gene to synthesize G1P and, consequently, the capacity to synthesize archaeal membrane
13 lipids. However, our analyses reveal their genetic capacity to synthesize G3P-based 'chimeric
14 lipids' with either two ether-bound isoprenoidal chains or with an ester-bound fatty acid instead of
15 an ether-bound isoprenoid. These archaea may reflect the 'archaea-to-eukaryote' membrane
16 transition stage which have led to the current 'lipid divide'.

17 Introduction

18 Membrane lipids are essential building blocks for the cell since membranes define the ‘inside’
19 and the ‘outside’ of the cell. Membranes are involved in many biological processes such as
20 establishing and maintaining trans-membrane gradients, compartmentalizing biochemical reactions
21 into distinct functional domains, controlling transport into and out of cells, and inter- and intra-
22 cellular communication. The membrane lipid composition is also one of the most remarkable traits
23 distinguishing the three domains of life, Archaea, Bacteria, and Eukarya (Woese and Fox, 1977).
24 Membrane lipids of Bacteria and Eukarya share a large number of structural similarities as they are
25 typically composed of two fatty acid chains that are linked to a glycerol moiety via ester bonds and
26 are organized in a bilayer structure (Lombard *et al.*, 2012a). On the other hand, membrane lipids of
27 Archaea are characterized by ether linkages between the glycerol moiety and isoprene-based alkyl
28 chains in either a bilayer or monolayer (Koga and Morii, 2007; Lombard *et al.*, 2012a). These traits
29 are not fully exclusive to these groups since membrane-spanning lipids have also been reported in
30 some members of the Bacteria (Sinninghe Damsté *et al.*, 2002, 2007; Weijers *et al.*, 2006), and fatty
31 acids in some archaeal species (Gattinger *et al.*, 2002). An exclusive distinction in the structures of
32 membrane lipids of archaea and bacteria/eukaryotes is the opposite stereochemistry of the glycerol
33 phosphate backbone, being *sn*-glycerol-1-phosphate (G1P) in archaea, and *sn*-glycerol-3-phosphate
34 (G3P) in bacteria and eukaryotes (Kates, 1993). The biosynthesis of G3P and G1P is catalyzed by
35 two entirely different enzymes (i.e. glycerol-1- and glycerol-3-phosphate dehydrogenase, G1PDH,
36 and G3PDH, respectively) that, based on differences in the catalytic reaction and protein sequence
37 (Koga *et al.*, 2003; Han *et al.*, 2005), are not evolutionary related (Koga *et al.*, 1998). This
38 differentiation of lipid structures between Archaea, on the one hand, and Bacteria and Eukarya, on
39 the other, has been coined as the ‘the lipid divide’.

40 This ‘lipid divide’ has posed some fundamental questions on microbial evolution. Since
41 Archaea and Bacteria are believed to stem from a common ancestor (the cenancestor or last
42 universal common ancestor, LUCA), their completely different membrane lipid structures represent
43 a conundrum. Koga *et al.* (Koga *et al.*, 1998) proposed that the cenancestor lacked a membrane and

44 that the specific archaeal and bacterial membrane lipid biosynthetic pathways emerged later and
45 independently in the lineages leading to Archaea and Bacteria. Martin & Russell (2003)
46 hypothesized that the cenancestor had mineral monosulfide compartments instead of lipids.
47 Wächtershäuser (2003) suggested that the cenancestor had a lipid heterochiral membrane containing
48 both stereochemical forms of the glycerol phosphate backbone, which progressively diverged into a
49 more stable homochiral membrane leading to the differentiation between archaea and bacterial
50 membranes. However, experiments with liposomes containing both archaeal and bacterial
51 membrane lipids showed that heterochiral membranes are also stable (Fan *et al.*, 1995; Shimada *et*
52 *al.*, 2011), suggesting that there exists no evolutionary pressure to select for organisms with a
53 homochiral membrane. A recent study by Sojo *et al.* (2014) based on modeling of membrane
54 bioenergetics suggested that LUCA did not have membranes with glycerol phosphate headgroups,
55 which would have reduced proton permeability, but rather a lipid bilayer composed of both fatty
56 acids and isoprenes, and that modern membranes in Bacteria and Archaea arose later and
57 independently.

58 Another conundrum is the similarity of membrane lipids of the Eukarya with those of Bacteria
59 rather than with those of the Archaea, which are believed to be the predecessors of the Eukarya
60 (Pereto *et al.*, 2004). According to the classical Woesean three-domain phylogeny, the last common
61 ancestor of archaea and eukaryotes would have had an archaeal membrane that was later replaced
62 by a bacterial-like membrane in eukaryotes, or alternatively that an ancestral mixed membrane with
63 G1P- and G3P-based membrane lipids evolved to an archaeal membrane in archaea and to a
64 bacterial-like membrane in eukaryotes. However, both options are difficult to reconcile as they
65 would involve an intensive horizontal gene transfer of the genes required, while the mixed
66 membrane model would imply that bacterial-like membranes evolved twice from the cenancestor in
67 bacteria and in eukaryote. Currently, the most accepted early life evolutionary theory considers
68 Archaea and Bacteria as primary branches derived directly from the cenancestor, while Eukarya
69 would have evolved secondarily as a chimeric organism derived from the endosymbiosis of one
70 bacterium (the ancestor of mitochondria) within a host cell (Gray and Doolittle, 1982; Golding and

71 Gupta, 1995; among others). However, the origin of the host cell is still under debate. In any case,
72 most models of the origin of eukaryotic cells require a transition from an archaeal-like membrane to
73 a bacterial membrane, including a reversal of the glycerol stereochemistry of membrane lipids
74 Nonetheless, no evidence for this kind of transition has ever been found in bacteria or archaea,
75 casting some doubts on this mechanism.

76 The growing availability of genomes could shed light on the evolutionary processes leading to
77 the 'lipid divide'. Recent studies based on environmental metagenomics have defined several new
78 archaeal lineages (Castelle *et al.*, 2015). Currently, the domain Archaea is represented by two
79 superphyla (DPANN and TACK) and the phylum Euryarchaeota (Guy and Ettema, 2011; Fig. S1).
80 The TACK-superphylum is comprised of Thaumarchaeota, Aigarchaeota, Crenarchaeota,
81 Korarchaeota, and some other phyla (e.g. Guy and Ettema, 2011; Williams *et al.*, 2012; Martijn and
82 Ettema, 2013). Some phylogenomic studies have provided evidence that the archaeal 'ancestor' of
83 the eukaryotic cell emerged from the TACK superphylum (Guy and Ettema, 2011). Furthermore, a
84 recent study suggests that the novel candidate archaeal phylum 'Lokiarchaeota' (Deep-Sea Archaeal
85 Group/Marine Benthic Group B, DSAG/MBG-B; Spang *et al.*, 2015; Fig. S1), a deep branching
86 clade of the TACK superphylum, forms a monophyletic group with the eukaryotes. Indeed, the
87 'Lokiarchaeum' composite genome codes a remarkable number of eukaryotic signature proteins,
88 supporting the hypothesis that the eukaryotic cell evolved from an archaeal ancestor of this group
89 (Spang *et al.*, 2015).

90 The recent discovery of Lokiarchaeum, which potentially shares a common ancestor with
91 eukaryotes, prompted us to re-examine the 'lipid divide' conundrum. We investigated two key
92 aspects of the lipid divide: the specific stereoconfiguration of archaeal lipids and the capacity for
93 fatty acid synthesis in archaea. We searched for homologs of genes encoding for enzymes involved
94 in membrane lipid and fatty acid biosynthetic pathways in archaeal genomes and performed
95 phylogenomic analyses with the annotated homologs. The results reveal differences in the lipid
96 biosynthetic pathway, especially concerning the stereochemistry of the glycerol phosphate

97 backbone, in certain uncultured archaeal groups at key evolutionary phylogenetic positions with
98 substantial implications for our understanding of the ‘lipid divide’.

99 **Results and Discussion**

100 *Enzymes involved in the glycerol phosphate stereospecific biosynthesis in Archaea*

101 The stereoconfiguration of archaeal lipids is established by the enzyme G1PDH. This enzyme is
102 thought to be restricted to archaea (e.g. Pereto *et al.*, 2004; Koga and Morii, 2007; Matsumi *et al.*,
103 2011) although a G1PDH homolog (AraM) has been found in *Bacillus* sp., and some related
104 bacterial species (Guldan *et al.*, 2008). Our survey of archaeal genomes revealed that the gene
105 coding for G1PDH (*egsA*, Fig.1) is present in almost all examined archaea but, interestingly, is
106 absent in marine group II euryarchaeota (MGII; Iverson *et al.*, 2012), in fosmid sequences of the
107 MGII and marine group III euryarchaeota (MGIII) (Deschamps *et al.*, 2014), ‘Lokiarchaeum’
108 (Spang *et al.*, 2015), and all examined species of the DPANN superphylum (Castelle *et al.*, 2015)
109 (Table 1, Table S1). This suggests that these uncultivated archaea may not have the ability to
110 synthesize the G1P backbone of archaeal lipids. For the members of the DPANN this is not
111 surprising because they have simplified genomes of reduced size and are thought to rely on host
112 cells or cell debris for the synthesis of their lipids (Waters *et al.*, 2003; Jahn *et al.*, 2004). In this
113 respect, it is notable that in some of the DPANN genomes some homologs of enzymes involved in
114 the archaeal membrane lipid biosynthesis are present, although they lack the MVK gene encoding
115 for mevalonate kinase (Table 1; Table S1), an essential enzyme for isoprenoid biosynthesis. This
116 situation may represent an intermediate stage of progressively losing those genes. However, truly
117 exceptional is the lack of G1PDH in MGII and MGIII euryarchaeota and in ‘Lokiarchaeum’, as we
118 found that genomes of these groups of archaea still harbor all the other known genes coding for the
119 enzymes of the archaeal lipid biosynthetic pathway (i.e. geranylgeranylgeranyl phosphate synthase,
120 GGGP; digeranylgeranylgeranyl phosphate synthase, DGGGP; geranyl reductase, GR, among
121 others; Table 1; Table S1, S2). It should be noted that the current genome assembly of
122 ‘Lokiarchaeum’ (*Lokiarchaeum* sp. GC14_75), is 92% complete (Spang *et al.*, 2015), and thus

123 there is a small chance that the gene coding for G1PDH would be located in the unsequenced part.
124 However, we also did not detect any homologs of the G1PDH coding gene in the larger
125 metagenome dataset (LCGC14AMP, 56.6 Gbp) reported in the same study (Spang *et al.*, 2015).
126 The lack of G1PDH homologs in the fosmid sequences of MGIII (Deschamps *et al.*, 2014) could
127 potentially be due to their lack of completeness, however this can be ruled out for the genome of
128 MGII reported by Iverson *et al.*, 2012, which is closed. Our analysis strongly suggests that MGII
129 and MGIII euryarchaeota and 'Lokiarchaeum' are capable of synthesizing isoprenoid-based ether
130 lipids for their membranes but not with G1P as the glycerol building block.

131 G3PDH (encoded by the *gps* gene) catalyzes the conversion of dihydroxyacetone phosphate
132 (DHAP) into G3P and this enzyme is responsible in Bacteria and Eukarya for the stereochemistry
133 of the glycerol units of their membrane lipids. *Gps*-coded G3PDH homologs were previously
134 detected in the euryarchaeota *Archaeoglobus fulgidus* and *Methanothermobacter*
135 *themoautotrophicum*, in addition to G1PDH, but their metabolic function is unknown (Pereto *et al.*,
136 2004). Some (heterotrophic) archaea have been reported to synthesize a 'G3PDH' enzyme encoded
137 by the *glp* gene (Pereto *et al.*, 2004; Koga and Morii, 2007) but this enzyme catalyzes the
138 conversion of G3P into DHAP, the reverse of the reaction catalyzed by *gps*-coded G3PDH (Fig. 1).
139 It is believed that this enables heterotrophic archaea to feed glycerol into the glycolysis pathway
140 (Nishihara *et al.*, 1999), as it is also observed for bacteria able to metabolize glycerol. These
141 heterotrophic archaea still biosynthesize membrane lipids with the archaeal stereochemistry as they
142 also harbor G1PDH (Fig. 1).

143 In our survey of archaeal genomes, *gps*-encoded G3PDH homologs were detected in MGII/III
144 euryarchaeota, and in some archaea of the orders Archaeoglobales and Methanobacteriales
145 (*Methanobrevibacter* sp.), as well as in species of the DPANN superphylum (AR9 and AR11
146 genomes of the Woesearchaeota), but not in 'Lokiarchaeum' (Table 1; Table S1). Homologs of *glp*-
147 encoded G3PDH were found in several archaeal genomes including members of the
148 Thermococcales, Archaeoglobales, Halobacteriales, Thermoplasmatales, Korarchaeota, some
149 Crenarchaeota genomes, as well as in the 'Lokiarchaeum' genome, which contains three putative

150 homologs of the enzyme (Table 1; Table S1, S2). To infer the evolutionary history of the annotated
151 archaeal G3PDH homologs, we constructed a phylogenetic tree including the archaeal *glp*- and *gps*-
152 coded G3PDH homologs, as well as bacterial and eukaryotic homologs (Fig. 2). The *glp*-coded
153 G3PDH archaeal homologs were mainly grouped in two main clusters with cluster 1 including
154 homologs of the Thermococcales, Thermoproteales, Desulfurococcales, Archaeoglobales, among
155 others, and cluster 2 comprising homologs of the Halobacteriales (Fig. 2A). Interestingly, the three
156 putative *glp*-coded G3PDH detected in the ‘Lokiarchaeum’ genome were closely related to bacterial
157 and eukaryotic G3PDH homologs (Fig. 2A). In addition, the *gps*-coded G3PDH archaeal homologs
158 do not form a monophyletic group (Fig. 2B), which may indicate horizontal gene transfer (HGT)
159 from bacteria to archaea in different independent events (Pereto *et al.*, 2004).

160 G3P is not only formed from DHAP by *gps*-coded G3PDH but also by phosphorylation of
161 glycerol catalyzed by glycerol kinase, encoded by the *glpK* gene (Fig. 1). We detected homologs of
162 the *glpK* gene in genomes of the euryarchaeota Thermococcales, Archaeoglobales, Halobacteriales,
163 and Thermoplasmatales, as well as in the genomes of the *Aciduliprofundum* and MGII/III groups,
164 and in genomes of the Korarchaeota and Crenarchaeota phyla (Table 1). Two putative homologs of
165 the gene encoding for the glycerol kinase were detected in the ‘Lokiarchaeum’ genome (Table 1;
166 Table S1, S2). The two putative homologs of ‘Lokiarchaeum’ annotated as glycerol kinases display
167 a XylB pentulose or hexulose kinase region. In order to confirm the identity of these homologs, we
168 constructed a phylogenetic tree including the glycerol kinase proteins previously described in
169 archaeal genomes and carbohydrate kinase proteins closely related to the annotated ‘Lokiarchaeum’
170 *glpK* (Fig. 3). The ‘Lokiarchaeum’ *glpK* homologs were closely related to carbohydrate kinases of
171 the euryarchaeon *Archaeoglobus fulgidus* and also to xylulose kinases of Bacteria, while the
172 glycerol kinases of archaeal genomes were grouped in another cluster (Fig. 3). Considering this
173 analysis, we cannot confirm the identity of the putative *glpK* coding genes annotated in the
174 ‘Lokiarchaeum’ genomes as true glycerol kinases based on their divergence with previously
175 characterized archaeal glycerol kinases.

176 G3P can also be synthesized by degradation of glycerophosphodiester by a
177 glycerophosphodiester phosphodiesterase (GDPD) producing the corresponding alcohols and G3P
178 (Larson *et al.*, 1983; Fig. 1). Glycerophosphodiester are enzymatically produced by
179 phospholipases A₁ and A₂ from membrane phospholipids (e.g. Istivan *et al.*, 2006).
180 Glycerophosphodiester phosphodiesterase activities have been characterized in bacteria as well as
181 in eukaryotes (Tommassen *et al.*, 1991; Fisher *et al.*, 2005; van der Rest *et al.*, 2002), and genomic
182 analyses have revealed a wide distribution of this protein family from bacteria and Archaea to
183 metazoans, plants, and fungi (Santelli *et al.*, 2004). In the bacterium *Escherichia coli*, the
184 transformation of glycerophosphodiester into G3P is thought to be catalyzed by two homologous
185 enzymes, a periplasmic GDPD GlpQ, and a cytosolic GDPD UgpQ with a broad substrate
186 specificity toward various glycerophosphodiester (e.g. Tommassen *et al.*, 1991). Here we detected
187 archaeal UgpQ homologs in genomes of the Crenarchaeota, and in euryarchaeotal genomes of the
188 Methanobacteriales, Thermococcales, Methanomicrobiales, Halobacteriales and
189 Thermoplasmatales (Table 1; Table S1). Two putative UgpQ GDPD homologs were also detected
190 in two genomes of the uncultured marine euryarchaeota group II/III, which were in turn closely
191 related to putative UgpQ GDPD of the euryarchaeota Halobacteriales (Fig. 4). In addition, two
192 putative homologs of UgpQ GDPD were detected in the 'Lokiarchaeum' genome (Table 1; Table
193 S1-S2), which were closely related to another putative UgpQ GDPD annotated in the DPANN
194 Woesearchaeota genome GW2011_AR3 as well as UgpQ detected in bacterial genomes of the
195 Thermotogae (Fig. 4). The detection of two putative GDPD UgpQ in the 'Lokiarchaeum' genome
196 opens the possibility of the formation of a G3P backbone by degradation of glycerophosphodiester,
197 as indicated in Fig. 1.

198 Putting this genetic evidence together, the data indicate that the unique archaeal groups that lack
199 the gene encoding for G1PDH, i.e. the MGII/III euryarchaeota and 'Lokiarchaeum', harbor
200 homologs of genes involved in the synthesis of the G3P backbone in Bacteria and Eukarya, either
201 through the catalysis of DHAP to G3P in the case of MGII/III euryarchaeota (G3PDH encoded by
202 *gps*), or in 'Lokiarchaeum' by degradation of glycerophosphodiester by glycerophosphodiester

203 phosphodiesterase (UgpQ GDPD) or by metabolism of glycerol into G3P via glycerol kinase
204 (encoded by the *gfpK* gene). Consequently, it is tempting to speculate that both MGII and MGIII
205 euryarchaeota and 'Lokiarchaeum' synthesize archaeal ether-linked membrane lipids, since they
206 have the complete set of the genes coding for the enzymes of the archaeal lipid biosynthetic
207 pathway (Table 1; Table S1, S2), but with the G3P stereochemistry typical for Bacteria and
208 Eukarya, as they lack genes for G1PDH but possess genes encoding for enzymes for G3P
209 formation. However, the synthesis of these kinds of lipids would be only possible if enzymes
210 similar to GGGP and DGGGP synthases would catalyze the formation of ether bonds between
211 isoprenoid chains and the G3P backbone as specified in the hypothetical pathway in Fig. 1.

212 *Enzymes involved in the fatty acid biosynthetic pathway in Archaea*

213 In bacterial fatty acid biosynthesis, the acetyl-CoA carboxylase (ACC) converts acetyl-
214 coenzyme A (CoA) into malonyl-CoA (Fig. 5). Secondly, the peptide cofactor acyl carrier protein
215 (ACP) has to be activated by an ACP synthase. Finally, the malonyl-CoA:ACP transacylase
216 (MCAT) charges the malonyl-CoA to holo-ACP, resulting in malonyl-ACP building blocks needed
217 by fatty acid synthases (Fig. 5). Although the occurrence of diacyl glycerols is generally believed to
218 be restricted to Bacteria and Eukarya, the presence of minor amounts of free fatty acids have been
219 previously reported in some archaea (Kates *et al.*, 1968; Langworthy *et al.*, 1974; Gattinger *et al.*,
220 2002). In line with this, homologs of several of bacterial enzymes of the fatty acid biosynthetic
221 pathway (i.e. ACC; beta-ketoacyl synthase, KAS, FabH; beta-ketoacyl reductase, KR, FabG; DH,
222 beta-hydroxyacyl dehydratase; and enoyl reductase, ER) have been detected in some archaeal
223 genomes (Pereto *et al.*, 2004; Fig. 5). In addition, a study by Iverson *et al.* (2012) annotated
224 homologs of the genes coding for ACC, KAS, KR, and ER in the genome of a MGII euryarchaeota.
225 Lombard *et al.* (2012b) observed that, except for a few unrelated species that probably acquired
226 ACP by independent HGT (i.e. some species of the Methanomicrobiales and Halobacteriales), no
227 homologs of the ACP-processing machinery (ACP synthase and MCAT) could be detected in
228 archaeal genomes. More recently, Dibrova *et al.* (2014) suggested a hypothetical archaeal fatty acid

229 pathway based on the presence of the gene coding for archaeal acetyl-CoA-acetyltransferase (also
230 known as acetyl-CoA C-acyl transferase) in all archaeal genomes up to date with the exception of
231 *Nanoarchaeum equitans* (Matsumi *et al.*, 2011). This enzyme catalyzes the first condensation
232 reaction in the mevalonate pathway producing acetoacyl-CoA, which then would be further reduced
233 and dehydrated by bacterial-type enzymes involved in the β -oxidation of fatty acids (acyl-CoA
234 dehydrogenase, FadE; enoyl-CoA hydratase, FadB1; 3-hydroxyacyl-CoA dehydrogenase, FadB2;
235 Fig. 5), operating in reverse direction.

236 To shed further light on the potential capacity of archaea to synthesize fatty acids we performed
237 an extensive search for archaeal homologs of the enzymes involved in the ACP-processing
238 machinery (i.e. ACP synthase and MCAT), which are generally lacking in archaeal genomes and
239 could potentially prohibit a complete the archaeal fatty acid biosynthesis. We also searched for
240 archaeal homologs of the beta-ketoacyl synthase (KAS), which have been previously annotated in
241 several archaeal genomes. Moreover, we also performed a more extensive search for the homologs
242 potentially involved in the hypothetical archaeal fatty acid synthesis pathway as proposed by
243 Dibrova *et al.*, (2014) in available archaeal genomes.

244 Putative homologs of ACP synthase were detected in some species of Methanomicrobiales,
245 Archaeoglobales, Halobacteriales, Thermoplasmatales, in some Crenarchaeota species, and in a
246 genome of a species in the DPANN superphylum (i.e. AR5 Aenigmarchaeota; Table 1; Table S1).
247 In our survey, we also detected MCAT (FabD) homologs in MGII and MGIII genomes (Table 1;
248 Table S1), as well as in some Halobacteriales (cf. Lombard *et al.*, 2012b). In the case of the MGII,
249 we detected the MCAT (FabD) gene as part of the previously annotated polyketide synthase, which
250 also contained a beta-ketoacyl synthase (KAS) and a polyketide synthase dehydratase (FabA/Z
251 dehydratase) domains. We have also observed this distribution of the MCAT (FabD) coding region
252 for several of the MGII/III genomes released by Deschamps *et al.* (2014) (Table 1; Table S1). In
253 addition, a putative MCAT homolog was also detected in the 'Lokiarchaeum' genome within the
254 protein previously annotated as phenol phthiocerol synthesis polyketide synthase type I (Table S1,
255 S2). This protein harbors a MCAT (FabD; comprised between residues 14604–15485; Table S2),

256 and KAS regions (FabBI and FabFII; residues 13674–14525). We performed phylogenetic analyses
257 of the MCAT (FabD) proteins detected in archaeal genomes to determine their evolutionary
258 relationships between each other and with bacterial homologs (Fig. 6). MCAT homologs of the
259 MGII and MGIII, and ‘Lokiarchaeum’ were related to bacterial MCAT homologs of the
260 Acidobacteria, Chloroflexi, and Firmicutes, while the MCAT homologs detected in Halobacteriales
261 genomes were quite different from the rest of the archaeal homologs as well as the bacterial ones,
262 suggesting a different evolutionary origin for these MCAT proteins.

263 Archaeal homologs of the genes coding for the acyl-CoA dehydrogenase FadE, enoyl-CoA
264 hydratase FadB1, and 3-hydroxyacyl-CoA dehydrogenase FadB2 were detected in some of the
265 genomes of the euryarchaeota Archaeoglobales, Halobacteriales, Thermoplasmatales, uncultured
266 marine euryarchaeota group II/III, MBG-D, and most of the Crenarchaeotal and Thaumarchaeotal
267 genomes (Table 1; Table S1). One putative homolog of FadE was detected in the ‘Lokiarchaeum’
268 genome, as well as multiple copies of putative homologs of FadB1 and FadB2 (Table 1; Table S1,
269 S2), which would also suggest that ‘Lokiarchaeum’ harbors the potential for fatty acid synthesis
270 with the hypothetical pathway proposed by Dibrova *et al.* (2014).

271 Our survey of the occurrence of genes coding for key fatty acid biosynthetic enzymes (i.e. ACP
272 synthase, MCAT and KAS) in archaeal genomes (Table 1; Table S1) suggests that only species of
273 the Halobacteria, MGII/III euryarchaeota and ‘Lokiarchaeum’ have all the key genes required to
274 potentially synthesize fatty acids. Species of the Halobacteria possess all three key genes (Table 1;
275 Table S1). Although MGII/III and ‘Lokiarchaeum’ lack annotated homologs of ACP synthase
276 (Table 1; Table S1), these archaeal groups could potentially still synthesize bacterial-like fatty acids
277 by an ACP-independent pathway as proposed by Lombard *et al.* (2012b). Furthermore, the
278 extensive search we performed for the genes coding for the FadE, FadB1 and FadB2, also showed
279 that most of the archaeal genomes, including MGII/III euryarchaeota and ‘Lokiarchaeum’, harbor
280 the potential for hypothetical fatty acid biosynthesis pathway proposed by Dibrova *et al.* (2014)
281 (Fig. 5).

282 Based on the genetic potential of some archaea to produce fatty acids, we further investigated
283 archaeal genomes for genes coding for enzymes catalyzing the esterification of fatty acids and G3P
284 required for the formation of glycerol ester lipids (Fig. 5). There are two families of enzymes
285 responsible for the acylation of the 1-position of the G3P. The PlsB acyltransferase, found in the
286 bacteria *Escherichia coli* and in many eukaryotes, primarily uses acyl-acyl carrier protein (ACP)
287 end products of fatty acid biosynthesis (acyl-ACP) as acyl donors but may also use acyl-CoA
288 derived from exogenous fatty acids (Fig. 5). The other family concerns the PlsY acyltransferase
289 which is more widely distributed in Bacteria and uses as donor acyl-phosphate produced from acyl-
290 ACP by the PlsX, an acyl-ACP:PO₄ transacylase enzyme (Fig. 5). The acylation in the 2-position
291 of the G3P is carried out by the 1-acylglycerol-3-phosphate *O*-acyltransferase (PlsC) (Fig. 5).

292 We performed genomic searches of putative archaeal homologs of the bacterial acyl-ACP
293 transferases involved in the formation of ester bonds between fatty acids and the G3P backbone in
294 the phospholipid synthesis (Fig. 5). No homologs of the PlsB acyltransferase were detected in any
295 of the archaeal genomes with the exception of one species of the DPANN superphylum (AR1
296 Pacearchaeota; Table 1; Table S1). Archaeal homologs to the PlsY acyltransferase were only found
297 in the 'Lokiarchaeum' genome (i.e. one putative PlsY homolog; Table 1; Table S1, S2). Molecular
298 phylogeny (Fig. 7) indicated that the 'Lokiarchaeum' PlsY homolog was closely related to PlsY
299 enzymes of bacterial groups such as Thermotogae, Spirochaetales and Dictyoglomales which
300 suggest that this enzyme was acquired by lateral gene transfer from Bacteria. A wide variety of
301 putative homologs of the PlsC 1-acylglycerol-3-phosphate *O*-acyltransferase were found in MGII
302 and MGIII genomes, a DPANN genome (AR11 Woesearchaeota), and two putative PlsC were
303 found in the 'Lokiarchaeum' genome (Table 1; Table S1, S2). Moreover, PlsC protein homologs of
304 the MGII/III euryarchaeota, AR11 DPANN, and 'Lokiarchaeum' were closely related to those of
305 the α -, β -Proteobacteria or Actinobacteria, the newly proposed Parcubacteria group (Brown *et al.*,
306 2015), and a species of the Firmicutes, respectively (Fig. 7).

307 Our data suggest that, in addition to the apparent ability to synthesize 'bacterial' G3P, MGII/III
308 euryarchaeota and 'Lokiarchaeum' also possess a putative fatty acid synthetic pathway.

309 Furthermore, the detection of homologs of the acyl transferase PlsY in the ‘Lokiarchaeum’ genome
310 and PlsC homologs in both MGII/III euryarchaeota and ‘Lokiarchaeum’ genomes suggests that
311 their biosynthetic machinery would be able to form ester-bonded fatty acid membrane lipids with
312 G3P stereochemistry. Based on the enzyme inventory (Table 1; Table S1), these archaea are
313 predicted to produce chimeric membrane lipids, such as di- or tetraether-linked isoprenoidal
314 membrane lipids with a bacterial/eukaryote G3P stereochemistry, or lipids with one ether-linked
315 isoprenoidal chain at position *sn*-1 of a G3P backbone and one ester-bound fatty acid at position *sn*-
316 2 (see “hypothetical part” of Fig. 1). Mixed ether/ester membrane lipids have been previously
317 detected in aerobic and anaerobic bacteria such as anammox bacteria, sulfate-reducing bacteria,
318 members of the bacterial order Thermotogales and Acidobacteria (Rütters *et al.*, 2001; Sinninghe
319 Damsté *et al.*, 2002, 2007, 2011, 2014). In fact, the presence of these types of lipids in the order
320 Thermotogales, an early-branching clade of the Bacteria, was interpreted as an indication that the
321 ability to produce both ether and ester-linked membrane lipids developed relatively early during
322 microbial evolution (Sinninghe Damsté *et al.*, 2007). However, the early branching in the tree of
323 life of Thermotogales and Aquificales has been questioned and it has even been proposed that the
324 majority of the genes of these groups shows affinities to Archaea and Firmicutes (Zhaxybayeva *et*
325 *al.*, 2009, among others).

326 In addition, ‘chimeric’ tetraether lipids containing both n-alkyl and isoprenoidal chains have
327 been previously detected in the environment (Schouten *et al.*, 2000; Liu *et al.*, 2012). In the case of
328 ‘Lokiarchaeum’, it is also possible that they synthesize bacterial-like fatty acids ester-bound at the
329 *sn*-1 and *sn*-2 positions of the G3P, as we have detected both putative acyltransferases (PlsY and
330 PlsC) in its genome. However, we did not detect a putative homolog of the PlsX protein involved in
331 the transformation of acyl-ACP to acylphosphate needed for the catalysis mediated by PlsY.
332 Therefore it remains unknown if ‘Lokiarchaeum’ is able to mediate the formation of bacterial-like
333 ester-bond fatty acid in the *sn*-1 position. The formation of the hypothetical chimeric tetraether
334 lipids (see “hypothetical part” of Fig. 1) would follow a biosynthetic pathway in which enzymes
335 similar to GGGP and DGGGP synthases would catalyze the formation of ether bonds between

336 isoprenoid chains and G3P backbone in *sn*-2 position instead of with the expected G1P. Since
337 GGGP synthase has proven to be selective for G1P (Peterhoff *et al.*, 2014), it would suggest that
338 this step is mediated by a totally different enzyme

339 *Implications for the 'lipid divide'*

340 The potential capacity of synthesis of isoprenoidal ether and fatty acid ester lipids with a G3P
341 backbone within a single organism, i.e. MGII/III euryarchaeota species and 'Lokiarchaeum', sheds
342 new light on the current 'lipid divide'. This is especially relevant for 'Lokiarchaeum' as its genome
343 codes a remarkable number of eukaryotic signature proteins, which has been used as an argument to
344 support the hypothesis that the eukaryotic cell evolved from an archaeal ancestor of this group
345 (Spang *et al.*, 2015). Our genome mining study suggests that 'Lokiarchaeum' has the biosynthetic
346 capacity to synthesize archaeal ether-linked and fatty acid ester linked membrane lipids with the
347 bacterial/eukaryotic G3P stereochemistry further supports the hypothesis of Spang *et al.* (2015). If
348 'Lokiarchaeum' was indeed a descendant of the archaeal ancestor leading to the eukaryotic cell,
349 then this ancestor may have possessed the capacity for both isoprenoidal ether and fatty acid ester
350 lipids with a G3P backbone. After the endosymbiosis of the archaeal ancestor with a bacterium, the
351 capacity for isoprenoid ether lipid synthesis may have been lost, leaving the fatty acids ester lipids
352 with a G3P backbone as the main membrane lipid.

353 It is not clear why phylogenetically distant archaeal groups such as MGII/III euryarchaeota and
354 'Lokiarchaeum' both harbor these particular lipid biosynthetic capacities. Extensive bacteria-to-
355 archaea gene transfer has occurred in MGII/III euryarchaeota, Thaumarchaeota, Halobacteria and
356 mesophilic methanogens (López-García *et al.*, 2004; Brochier-Armanet *et al.*, 2011; Nelson-Sathi *et al.*
357 *et al.*, 2012; Deschamps *et al.*, 2014). It has been proposed that this has promoted their adaptation to a
358 mesophilic lifestyle (López-García *et al.*, 2015). The Lokiarchaeum genome also contains a
359 relatively high fraction of genes that display a high similarity to genes of bacterial origin (i.e. 29%
360 of all genes; Spang *et al.*, 2015), which is comparable to that in MGII/III euryarchaeota
361 (Deschamps *et al.*, 2014). This high level inter-domain gene exchange between Bacteria and

362 Archaea may have substantially impacted the membrane lipid biosynthetic pathway in both
363 MGII/III euryarchaeota and 'Lokiarchaeum' to such an extent that they produce 'chimeric'
364 membrane lipids. Acquisition of only one more bacterial gene (PlsB) by an ancestor of
365 'Lokiarchaeum' would result in a 'full' bacterial/eukaryotic lipid membrane pathway, paving the
366 road leading to the development of a 'truly' eukaryotic cell membrane. Our study suggests that the
367 'lipid divide' between the domain Archaea, on the one hand, and those of the Bacteria and Eukarya,
368 on the other, is less clear cut as previously thought.

369 The required next step following our phylogenomic study is to provide confirmation of our
370 hypothesis by identification of the 'chimeric' lipids predicted here. However, such an endeavor is
371 strongly hindered by the lack of cultivated representatives of MGII/III euryarchaeota and
372 'Lokiarchaeota'. Future studies should focus on determining 'unusual' membrane lipids in natural
373 environments with high abundances of these uncultured archaeal groups, in particular by
374 determining the stereochemistry of their glycerol membrane lipids (cf. Weijers *et al.*, 2006). This
375 may also provide further insight in the evolution of Eukarya from the prokaryotes.

376 **Experimental procedures**

377 *Computational analysis*

378 Putative homologs of the enzymes mentioned in the text (Table 1; Table S1, S2) were detected by
379 tblastn (search translated nucleotide databases using a protein query) and blastp (protein query
380 against protein databases) searches using annotated enzymes as query sequences and with a
381 minimum e-value of $1e^{-25}$. The identity of the putative homologs was further investigated by visual
382 inspection of the alignment.

383 *Phylogenetic analyses*

384 Putative and annotated partial homologs aligned by Muscle (Edgar, 2004) in Mega6 software
385 (Tamura *et al.*, 2013) and edited manually. Phylogenetic reconstruction was performed by
386 maximum likelihood in PhyML v3.0 (Guindon *et al.*, 2010) using the best model according to AIC
387 indicated by ProtTest 2.4 (Abascal *et al.*, 2005) as indicated in the figure legends.

388 **References**

- 389 Abascal, F., Zardoya, R., and Posada, D. (2005) ProtTest: Selection of best-fit models of protein
390 evolution. *Bioinformatics* 21: 2104-2105.
- 391 Boucher, Y., Kamekura, M, and Doolittle, W.F. (2004) Origins and evolution of isoprenoid lipid
392 biosynthesis in archaea. *Mol Microbiol* 52: 515-527.
- 393 Brochier-Armanet, C., Forterre, P., and Gribaldo, S. (2011) Phylogeny and evolution of the
394 Archaea: one hundred genomes later. *Curr Opin Microbiol* 3: 274-281.
- 395 Brown, C.T., Hug, L.A., Thomas, B.C., Sharon, I., Castelle, C.J., Singh, A., Wilkins, M.J.,
396 Wrighton, K.C., Williams, K.H., and Banfield, J.F. (2015) Unusual biology across a group
397 comprising more than 15% of domain Bacteria. *Nature* 523: 208-211.
- 398 Castelle, C.J., Wrighton, K.C., Thomas, B.C., Hug, L.A., Brown, C.T., Wilkins, M.J., Frischkorn,
399 K.R., Tringe, S.G., Singh, A., Markillie, L.M., Taylor, R.C., Williams, K.H., and Banfield, J.F.
400 (2015) Genomic expansion of domain archaea highlights roles for organisms from new phyla in
401 anaerobic carbon cycling. *Curr Biol* 25: 690-701.
- 402 Deschamps, P., Zivanovic, Y., Moreira, D., Rodriguez-Valera, F., and López-García, P. (2014)
403 Pangenome evidence for extensive interdomain horizontal transfer affecting lineage core and shell
404 genes in uncultured planktonic thaumarchaeota and euryarchaeota. *Genome Biol Evol* 6: 1549-
405 1563.
- 406 Dibrova, D.V., Galperin, M.Y., and Mulkidjanian, A.Y. (2014) Phylogenomic reconstruction of
407 archaeal fatty acid metabolism. *Environ Microbiol* 16: 907-918.
- 408 Edgar, R.C. (2004) MUSCLE: a multiple sequence alignment method with reduced time and space
409 complexity. *BMC Bioinformatics* 5: 113.
- 410 Fan, Q., Relini A., Cassinadri, D., Gambacorta, A., and Gliozzi, A. (1995) Stability against
411 temperature and external agents of vesicles composed of archaeal bolaform lipids and egg PC.
412 *Biochim Biophys Acta* 1240: 83-88.
- 413 Fisher, E., Almaguer, C., Holic, R., Griac, P., and Patton-Vogt, J. (2005) Glycerophosphocholine-
414 dependent growth requires Gde1p (YPL110c) and Git1p in *Saccharomyces cerevisiae*. *J Biol Chem*
415 280: 36110-36117.
- 416 Gattinger, A., Schloter, M., and Munch, J. C. (2002) Phospholipid etherlipid and phospholipid fatty
417 acid fingerprints in selected euryarchaeotal monocultures for taxonomic profiling. *FEMS Microbiol*
418 *Lett* 213: 133-139.
- 419 Golding, G.B., and Gupta, R.S. (1995) Protein-based phylogenies support a chimeric origin for the
420 eukaryotic genome. *Mol Biol Evol* 12: 1-6.
- 421 Gray, M., and Doolittle, W.F (1982) Has the endosymbiont hypothesis being proven? *Microbiol*
422 *Rev* 46: 1-42.
- 423 Guindon, S., Dufayard, J.F., Lefort, V., Anisimova, M., Hordijk, W., and Gascuel, O. (2010) New
424 algorithms and methods to estimate maximum-likelihood phylogenies: assessing the performance of
425 PhyML 3.0. *Syst Biol* 59: 307-321.
- 426 Guldan, H., Sterner, R., and Babinger, P. (2008) Identification and characterization of a bacterial
427 glycerol-1-phosphate dehydrogenase: Ni²⁺ dependent AraM from *Bacillus subtilis*. *Biochem* 47:
428 7376-7384.
- 429 Guy, L., and Ettema, T.J. (2011) The archaeal 'TACK' superphylum and the origin of eukaryotes.
430 *Trends Microbiol* 19: 580-587.

- 431 Han, J-S., and Ishikawa, K (2005) Active site of Zn⁽²⁺⁾-dependent sn-glycerol-1-dehydrogenase
432 from *Aeropyrum pernix* K1. *Archaea* 1: 311-317.
- 433 Istivan, T.S., and Coloe, P.J. (2006) Phospholipase A in Gram-negative bacteria and its role in
434 pathogenesis. *Microbiology* 152: 1263-1274.
- 435 Iverson, V., Morris, R.M., Frazar, C.D., Berthiaume, C.T., Morales, R.L., and Armbrust, E.V.
436 (2012) Untangling genomes from metagenomes: revealing an uncultured class of marine
437 Euryarchaeota. *Science* 335: 587-590.
- 438 Jahn, U., Summons, R., Sturt, H., Grosjean, E., and Huber, H. (2004) Composition of the lipids of
439 *Nanoarchaeum equitans* and their origin from its host *Ignicoccus* sp. strain KIN4/I. *Archiv*
440 *Microbiol* 182: 404-413.
- 441 Jung, M.Y., Park, S.J., Kim, S.J., Kim, J.G., Sinninghe Damsté, J.S., Jeon, C.O., and Rhee, S.K.
442 (2014) A mesophilic, autotrophic, ammonia-oxidizing archaeon of thaumarchaeal group I.1a
443 cultivated from a deep oligotrophic soil horizon. *Appl Environ Microbiol* 80: 3645-3655.
- 444 Kates, M. (1993) in *Membrane lipids of archaea, The biochemistry of Archaea (Archaeobacteria)*. D.
445 J. Kushner, D.J., and Matheson, A.T. eds. (Elsevier Science Publishers B.V., Amsterdam, The
446 Netherlands), p. 261-295.
- 447 Kates, M., Wassef, M.K., and Kushner, D.J. (1968) Radioisotopic studies on the biosynthesis of the
448 glyceryl diether lipids of *Halobacterium cutirubrum*. *Can J Biochem* 46: 971-977.
- 449 Koga, Y., and Morii, H. (2007) Biosynthesis of ether-type polar lipids in archaea and evolutionary
450 considerations. *Microbiol Mol Biol Rev* 71: 97-120.
- 451 Koga, Y., Kyuragi, T., Nishihara, M., and Sone, N. (1998) Did archaeal and bacterial cells arise
452 independently from non-cellular precursors? A hypothesis stating that the advent of membrane
453 phospholipid with enantiomeric glycerol phosphate backbones caused the separation of the two
454 lines of descent. *J Mol Evol* 47: 631.
- 455 Koga, Y., Sone, N., Noguchi, S., and Morii, H. (2003) Transfer of pro-R hydrogen from NADH to
456 dihydroxyacetonephosphate by sn-glycerol-1-phosphate dehydrogenase from the archaeon
457 *Methanothermobacter thermoautotrophicus*. *Biosci Biotechnol Biochem* 67: 1605-1608.
- 458 Langworthy, T.A., Mayberry, W.R., and Smith, P.F. (1974) Long-chain glycerol diether and polyol
459 dialkyl glycerol triether lipids of *Sulfolobus acidocaldarius*. *J Bacteriol* 119: 106-116.
- 460 Larson, T.J., Ehrmann, M., and Boos, W. (1983) Periplasmic glycerophosphodiester
461 phosphodiesterase of *Escherichia coli*, a new enzyme of the *glp* regulon. *J Biol Chem* 258: 5428-
462 5432.
- 463 Lebedeva, E.V., Hatzepichler, R., Pelletier, E., Schuster, N., Hauzmayer, S., Bulaev, A.,
464 Grigor'eva, N.V., Galushko, A., Schmid, M., Palatinszky, M., Le Paslier, D., Daims, H. and
465 Wagner, M. (2013) Enrichment and genome sequence of the group I.1a ammonia-oxidizing
466 Archaeon "*Ca. Nitrosotenuis uzonensis*" representing a clade globally distributed in thermal
467 habitats. *PLoS One* 8: e80835.
- 468 Liu, X.L., Summons, R.E., and Hinrichs, H.U. (2012) Extending the known range of glycerol ether
469 lipids in the environment: structural assignments based on tandem mass spectral fragmentation
470 patterns. *Rapid Commun Mass Spectrom* 26: 2295-2302.
- 471 Lloyd, K.G., Schreiber, D.G., Petersen, D.G., Kjeldsen, K.U., Lever, M.A., Steen, A.D.,
472 Stepanauskas, R., Richter, M., Kleindienst, S., Lenk, S., Schramm, A., and Jørgensen, B.B. (2013)
473 Predominant archaea in marine sediments degrade detrital proteins. *Nature* 496: 215-218.
- 474 Lombard, J., López-García, P., and Moreira, D. (2012a) The early evolution of lipid membranes
475 and the three domains of life. *Nat Rev Microbiol* 10: 507-515.

- 476 Lombard, J., López-García, P., and Moreira, D. (2012b) Phylogenomic investigation of
477 phospholipid synthesis in archaea. *Archaea* 2012: 630910.
- 478 López-García, P., Brochier, C., Moreira, D., and Rodríguez-Valera, F. (2004) Comparative analysis
479 of a genome fragment of an uncultivated mesopelagic crenarchaeote reveals multiple horizontal
480 gene transfers. *Environ Microbiol* 6: 19-34.
- 481 López-García, P., Zivanovic, Y., Deschamps, P., and Moreira, D. (2015) Bacterial gene import and
482 mesophilic adaptation in archaea. *Nat Rev Microbiol* 13: 447-456.
- 483 Martijn, J., and Ettema, T.J.G. (2013) From archaeon to eukaryote: the evolutionary dark ages of
484 the eukaryotic cell. *Biochem Soc Trans* 41: 451-457.
- 485 Martin, W., and Russell, M.J. (2003) On the origins of cells: a hypothesis for the evolutionary
486 transitions from abiotic geochemistry to chemoautotrophic prokaryotes, and from prokaryotes to
487 nucleated cells. *Philos Trans R Soc Lond B Biol Sci* 358: 59-83.
- 488 Matsumi, R., Atomi, H., Driessen, A.J., and van der Oost, J. (2011) Isoprenoid biosynthesis in
489 Archaea--biochemical and evolutionary implications. *Res Microbiol* 162: 39-52.
- 490 Nelson-Sathi, S., Dagan, T., Janssen, A., Steel, M., McInerney, J.O., Deppenmeier, U., and Martin,
491 W.F. Acquisition of 1,000 eubacterial genes physiologically transformed a methanogen at the origin
492 of Haloarchaea. *Proc Natl Acad Sci USA* 109: 20537-20542.
- 493 Nishihara, M., Yamazaki, T., Oshima, T., and Koga, Y. (1999) sn-Glycerol-1-phosphate-forming
494 activities in archaea: separation of archaeal phospholipid biosynthesis and glycerol catabolism by
495 glycerophosphate enantiomers. *J Bacteriol* 181: 1330-1333.
- 496 Pereto, J., Lopez-Garcia, P., and Moreira, D. (2004) Ancestral lipid biosynthesis and early
497 membrane evolution. *Trends Biochem Sci* 29: 469-477.
- 498 Peterhoff, D., Beer, B., Rajendran, C., Kumpula, E.P., Kapetaniou, E., Guldan, H., Wierenga, R.K.,
499 Sterner, R., and Babinger, P. (2014) A comprehensive analysis of the geranylgeranyl glyceryl
500 phosphate synthase enzyme family identifies novel members and reveals mechanisms of substrate
501 specificity and quaternary structure organization. *Mol Microbiol* 92: 885-899.
- 502 Rütters, H., Sass, H., Cypionka, H., and Rullkotter, J. (2001) Monoalkylether phospholipids in the
503 sulfate-reducing bacteria *Desulfosarcina variabilis* and *Desulforhabdus amnigenus*. *Arch Microbiol*
504 176: 435-442.
- 505 Santelli, E., Schwarzenbacher, R., McMullan, D. et al. (2004) Crystal structure of a
506 glycerophosphodiester phosphodiesterase (GDPD) from *Thermotoga maritima* (TM1621) at 1.60 Å
507 resolution. *Proteins* 56: 167-170.
- 508 Santoro, A.E., Dupont, C.L., Richter, R.A., Craig, M.T., Carini, P., McIlvin, M.R., Yang, Y., Orsi,
509 W.D., Moran, D.M., and Saito, M.A. (2015) Genomic and proteomic characterization of
510 "Candidatus Nitrosopelagicus brevis": an ammonia-oxidizing archaeon from the open ocean. *Proc*
511 *Natl Acad Sci USA* 112: 1173-1178.
- 512 Schouten, S., Hopmans, E.C., Pancost, R.D., and Damsté, J.S. (2000) Widespread occurrence of
513 structurally diverse tetraether membrane lipids: evidence for the ubiquitous presence of low-
514 temperature relatives of hyperthermophiles. *Proc Natl Acad Sci USA* 97: 14421-14426.
- 515 Shimada, H., and Yamagishi, A. (2011) Stability of heterochiral hybrid membrane made of
516 bacterial sn-G3P lipids and archaeal sn-G1P lipids. *Biochem* 50: 4114-4120.
- 517 Sinninghe Damsté, J. S., Rijpstra, W.I., Hopmans, E.C., Schouten, S., Balk, M., and Stams, A.J.
518 (2007) Structural characterization of diabolic acid-based tetraester, tetraether and mixed ether/ester,
519 membrane-spanning lipids of bacteria from the order Thermotogales. *Arch Microbiol.* 188: 629-
520 641.

- 521 Sinninghe Damsté, J.S., Rijpstra, W.I., Hopmans, E.C., Foesel, B.U., Wüst, P.K., Overmann, J.,
522 Tank, M., Bryant, D.A., Dunfield, P.J., Houghton, K., and Stott, M.B. (2014) Ether- and ester-
523 bound iso-diabolic acid and other lipids in members of acidobacteria subdivision 4. *Appl Environ*
524 *Microbiol* 80: 5207-5218.
- 525 Sinninghe Damsté, J.S., Rijpstra, W.I., Hopmans, E.C., Weijers, J.W., Foesel, B.U., Overmann, J.,
526 and Dedysh, S.N. (2011) 13,16-Dimethyl octacosanedioic acid (iso-diabolic acid), a common
527 membrane-spanning lipid of Acidobacteria subdivisions 1 and 3. *Appl Environ Microbiol* 77: 4147-
528 4154.
- 529 Sinninghe Damsté, J.S., Strous, M., Rijpstra, W.I., Hopmans, E.C., Geenevasen, J.A., van Duin,
530 A.C., van Niftrik, L.A., and Jetten, M. (2002) Linearly concatenated cyclobutane lipids form a
531 dense bacterial membrane. *Nature* 419: 708-712.
- 532 Sojo, V., Pomiankowski, A., and Lane, N. (2014) A bioenergetic basis for membrane divergence in
533 archaea and bacteria. *PLoS Biol.* 12: e1001926.
- 534 Spang, A., Saw, J.H., Jørgensen, S.L., Zaremba-Niedzwiedzka, K., Martijn, J., Lind, A.E., van Eijk,
535 R., Schleper, C., Guy, L., and Ettema, T.J. (2015) Complex archaea that bridge the gap between
536 prokaryotes and eukaryotes. *Nature* 521: 173-179.
- 537 Tamura, K., Stecher, G., Peterson, D., Filipinski, A., and Kumar, S. (2013) MEGA6: Molecular
538 Evolutionary Genetics Analysis version 6.0. *Mol Biol Evol* 30: 2725-2729.
- 539 Tommassen, J., Eiglmeier, K., Cole, S.T., Overduin, P., Larson, T.J., and Boos, W. (1991)
540 Characterization of two genes, *glpQ* and *ugpQ*, encoding glycerophosphoryl diester
541 phosphodiesterases of *Escherichia coli*. *Mol Gen Genet* 226: 321-327.
- 542 van der Rest, B., Boisson, A.M., Gout, E., Bligny, R., and Douce, R. (2002)
543 Glycerophosphocholine metabolism in higher plant cells. Evidence of a new glyceryl-
544 phosphodiester phosphodiesterase. *Plant Physiol* 130: 244-255.
- 545 Villanueva, L., Schouten, S., and Sinninghe Damsté, J.S. (2014) A Re-evaluation of the Archaeal
546 Membrane Lipid Biosynthetic Pathway. *Nat Rev Microbiol* 12: 438-448.
- 547 Wächtershäuser, G. (2003) From pre-cells to Eukarya—a tale of two lipids. *Mol Microbiol* 47: 13-
548 22.
- 549 Waters, E., Hohn, M.J., Ahel, I., Graham, D.E., Adams, M.D., Barnstead, M., Beeson, K.Y., Bibbs,
550 L., Bolanos, R., Keller, M., Kretz, K., Lin, X., Mathur, E., Ni, J., Podar, M., Richardson, T., Sutton,
551 G.G., Simon, M., Soll, D., Stetter, K.O., Short, J.M., and Noordewier, M. (2003) The genome of
552 *Nanoarchaeum equitans*: insights into early archaeal evolution and derived parasitism. *Proc Natl*
553 *Acad Sci USA* 100: 12984-12988.
- 554 Weijers, J. W., Schouten, S., Hopmans, E.C., Geenevasen, J.A., David, O.R., Coleman, J. M.,
555 Pancost, R.D., and Sinninghe Damsté, J.S. (2006) Membrane lipids of mesophilic anaerobic
556 bacteria thriving in peats have typical archaeal traits. *Environ Microbiol* 8: 648-655.
- 557 Williams, T.A., Foster, P.G., Nye, T.M.W., Cox, C.J., and Embley, T.M. (2012) A congruent
558 phylogenomic signal places eukaryotes within the Archaea. *Proc Royal Soc B* 279: 4870-4879.
- 559 Woese, C.R, and Fox, G.E. (1977) Phylogenetic structure of the prokaryotic domain: The primary
560 kingdoms. *Proc Natl Acad Sci USA* 74: 5088-5090.
- 561 Zhaxybayeva, O., Swithers, K.S., Lapierre, P., Fournier, G.P., Bickhart, D.M., DeBoy, R.T.,
562 Nelson, K.E., Nesbø, C.L., Doolittle, W.F., Gogarten, J.P., and Noll, K.M. (2009) On the chimeric
563 nature, thermophilic origin, and phylogenetic placement of the Thermotogales. *Proc Natl Acad Sci*
564 *U S A.* 106: 5865-5870.

565 **Acknowledgments**

566 This research was supported by the SIAM Gravitation Grant 024.002.002 from the Dutch Ministry
567 of education, Culture, and Science (OCW. Author contributions: L.V. and J.S.S.D. conceived the
568 study. L.V. was responsible for data processing, and analysis. All authors contributed to data
569 interpretation, formulation of hypotheses, and the writing of the paper. The authors do not have any
570 conflict of interest to declare.

For Peer Review Only

Table 1. Presence (√ in green) and absence (× in red) of archaeal homologs of enzymes related to membrane lipid biosynthesis, glycerol catabolism, and enzymes involved in fatty acid and mono- and diacyl glycerol biosynthesis (see Figure 1 and 5). Enzymes studied: MVK, Mevalonate kinase; G1PDH, Glycerol-1-phosphate dehydrogenase; G3PDH, Glycerol-3-phosphate dehydrogenase; *glpK*, glycerol kinase; GDPD, glycerophosphodiester phosphodiesterase; GGGP, geranylgeranyl glyceryl phosphate synthase (see archaeal GGGP synthase phylogenetic tree in Fig. S2), DGGGP, digeranylgeranyl glyceryl phosphate synthase (phylogenetic tree in Fig. S3); GR, geranylgeranyl reductase; FabD, MCAT Malonyl-coA:ACP-transacylase; KAS, beta-ketoacyl synthase; FadE, Acyl-CoA dehydrogenase; FadB1, Enoyl-CoA hydratase; FadB2, 3-hydroxyacyl-CoA dehydrogenase; PlsB, glycerol-3-phosphate *O*-acyltransferase; PlsY, glycerol-3-phosphate acyltransferase; PlsC, 1-acylglycerol-3-phosphate *O*-acyltransferase. For a complete overview see Table S1.

Phylogenetic classification	%**	Isoprenoid biosynthesis	Glycerol backbone biosynthesis		Glycerol & glycerol phosphodiester catabolism			Ether lipid production (ether bond formation & saturation of isoprenoids)			Fatty acid biosynthesis						Ester-bond formation glycerol and fatty acids		
		MVK	G1PDH	G3PDH <i>gps</i>	G3PDH <i>glp</i>	<i>glpK</i>	GDPD	GGGP	DGGGP	GR	ACP synthase	FabD	KAS	FadE	FadB1	FadB2	PlsB	PlsY	PlsC
EURYARCHAEOTA																			
Methanococcales	100	√	√	×	×	×	×	√	√	√	×	×	×	×	×	×	×	×	×
Methanobacteriales	100	√	√	√	×	×	√	√	√	√	×	×	×	×	×	×	×	×	×
Thermococcales	100	√	√	×	√	√	√	√	√	√	×	×	×	×	×	×	×	×	×
Methanosarcinales	100	√	√	×	×	×	×	√	√	√	×	×	×	×	√	×	×	×	×
Methanomicrobiales	100	√	√	×	×	×	√	√	√	√	√	×	×	×	×	×	×	×	×
Archaeoglobales	100	√	√	√	√	√	×	√	√	√	√	×	√	√	√	√	×	×	×
Halobacteriales	100	√	√	×	√	√	√	√	√	√	√	√	×	√	√	√	×	×	×
Thermoplasmatales																			
Thermoplasmata	100	√	√	×	√	√	√	√	√	√	√	×	×	√	×	√	×	×	×
Unclassified																			
<i>Aciduliprofundum</i>	100	√	√	×	√	√	√	√	√	√	×	×	×	×	×	×	×	×	×
Marine group II/III†	100	√	×	√	×	√	√	√	√	√	×	√	√	√	√	√	×	×	√
MBG-D‡	70	×	√	×	×	×	×	√	√	√	×	×	×	√	√	√	×	×	×
AIGARCHAEOTA																			
<i>Ca. Caldiarchaeum subterraneum</i>	100	√	√	×	×	×	×	√	√	√	×	×	×	√	√	√	×	×	×
KORARCHAEOTA																			
<i>Ca. Korarchaeum cryptofilum</i>	100	√	√	×	√	√	×	√	√	√	×	×	×	√	×	√	×	×	×

CRENARCHAEOTA																			
Sulfolobales	100	√	√	×	×	√	√	√	√	√	√	×	×	√	√	√	×	×	×
Desulfurococcales	100	√	√	×	√	√	√	√	√	√	√	×	×	√	√	√	×	×	×
Acidilobales	100	√	√	×	×	×	×	√	√	√	×	×	×	√	×	√	×	×	×
Thermoproteales	100	√	√	×	√	√	√	√	√	√	√	×	√	√	√	√	×	×	×
THAUMARCHAEOTA																			
Cenarchaeales	100	√	√	×	×	×	×	√	?	√	×	×	×	×	√	√	×	×	×
Nitrosopumilales	100	√	√	×	×	×	×	√	?	√	×	×	×	√	√	√	×	×	×
Nitrososphaerales	100	√	√	×	×	×	×	√	?	√	×	×	×	√	√	√	×	×	×
Unclassified§	100	√	√	×	×	×	×	√	?	√	×	×	×	√	√	√	×	×	×
DSAG/MBG-B#																			
Lokiarchaeum	92	√	×	×	√	√	√	√	√	√	×	√	√	√	√	√	×	√	√
DPANN¶																			
Diapherotrites																			
<i>Ca. Iainarchaeum andersonii</i>	88.5	×	×	×	×	×	×	√	×	√	×	×	×	×	×	×	×	×	×
AR10	100	×	×	×	×	×	×	√	×	√	×	×	×	×	×	×	×	×	×
Woesearchaeota																			
AR20	100	×	×	×	×	×	×	×	×	√	×	×	×	×	×	×	×	×	×
AR3	63	×	×	×	×	×	√	×	×	×	×	×	×	×	×	×	×	×	×
AR9	76	×	×	√	×	×	×	×	×	×	×	×	×	×	×	×	×	×	×
AR11	76	×	×	√	×	×	×	×	×	×	×	×	×	×	×	×	×	×	√
Pacearchaeota																			
AR19	91	×	×	×	×	×	×	×	×	×	×	×	×	×	×	×	×	×	×
AR1	89	×	×	×	×	×	×	×	×	×	×	×	×	×	×	×	√	×	×
Aenigmarchaeota																			
AR5	93	×	×	×	×	×	×	×	×	√	√	×	×	×	×	×	×	×	×
Micrarchaeota																			
<i>Ca. Micrarchaeum acidiphilum</i>	100	×	×	×	×	×	×	×	×	×	×	×	×	×	×	√	×	×	×
Nanoarchaeota																			
<i>Nanoarchaeum equitans</i>	100	×	×	×	×	×	×	×	×	×	×	×	×	×	×	×	×	×	×

*Refers to the apparent lack of DGGGP synthases in the genomes of Thaumarchaeota; Villanueva *et al.*, 2014; **Percentage of completeness of the (meta)genome; † Marine group II and III euryarchaeota genomes including MGII amplified from surface water (CM001443.1; Iverson *et al.*, 2012), marine group II euryarchaeote SCGC AB-629-J06 (NZ_AQVM00000000.1), Marine Group III euryarchaeote SCGC AAA288-E19 (AQT00000000.1), and sequences obtained by Deschamps *et al.* (2014). Only the MGII genome reported by Iverson *et al.*, 2012 is closed; ‡MBG-D, Marine Benthic Group D, SCGC AB-539-N05 (ALXL00000000) by Lloyd *et al.* (2013); §Unclassified Thaumarchaeota include *Ca. Nitrosopelagicus brevis* (GCA_000812185.1; Santoro *et al.*, 2015); *Ca. Nitrosoterrus chungbukensis* (AVSQ01000000; Jung *et al.*, 2014), and *Ca. Nitrosotenuis uzonensis* (CBTY000000000; Lebedeva *et al.*, 2013); #DSAG/MBG-B, Deep-Sea Archaeal Group/Marine Benthic Group-B, composite genome 'Lokiarchaeum' by Spang *et al.* (2015); ¶ DPANN superphylum including the metagenomes described in Castelle *et al.* (2015).

For Peer Review Only

Figure legends

FIGURE 1. Overview of the known and hypothetical diether and ether/ester lipid biosynthetic pathway in Archaea and the related pathway of glycerol metabolism. Autotrophic Archaea produce G1P, which is subsequently incorporated into archaeal membrane lipids, from GAP via DHAP (orange arrows). The glycerol metabolism pathway of heterotrophic Archaea, which feeds glycerol into the glycolysis pathway, is indicated with blue arrows. The green arrows indicate the here-proposed formation of G3P from DHAP by *gps*-coded G3PDH, commonly only found in Bacteria and Eukarya, and the formation of G3P from the degradation of glycerophosphodiester by a glycerophosphodiester phosphodiesterase (GDPD) (see text for details). Some other reactions are also performed by these organisms as indicated (B= Bacteria; E= Eukarya). Arrows in gradient orange/blue indicate steps performed by both auto- and heterotrophic archaea. **Purple triangles indicate putative homologs in the ‘Lokiarchaeum’ and/or MGII/III genomes (Table 1).** Steps included in the dashed line box are hypothetical and based on the predicted occurrence of specific enzymes (Table 1; Table S1) as discussed in the text. The names of enzymes are underlined and in case where the genes encoding for these enzymes have specific names they are given in italics. Abbreviations used: GAP, d-Glyceraldehyde-3-phosphate; G1P, Glycerol-1-phosphate; G3P, Glycerol-3-phosphate; GGGP, geranylgeranylglyceryl phosphate; DGGGP, digeranylgeranylglyceryl phosphate; DHAP, Dihydroxyacetone phosphate; G1PDH, glycerol-1-phosphate dehydrogenase; G3PDH, glycerol-3-phosphate dehydrogenase. “?” indicates an hypothetical enzyme similar to GGGP synthase but with a G3P stereo-chemistry as indicate din the text. ‘DGGGP synthase’ and ‘PlsC’ indicate hypothetical enzymes that are expected to perform a similar reaction to the original ones.

FIGURE 2. Phylogenetic tree of *sn*-glycerol-3-phosphate dehydrogenases (G3PDH). The tree clearly reveals two main clusters of G3PDH encoded by the *glp* (A) and *gps* (B) genes. These different forms of G3PDH catalyze the conversion of G3P into DHAP and the reverse reaction, respectively (see Fig. 1). *Glp*-coded G3PDH is common in Bacteria, Eukarya and Archaea, where it is one of the enzymes involved in feeding glycerol into the glycolysis pathway. The putative *glp*-G3PDH homologs found in the composite ‘Lokiarchaeum’ genome (Spang *et al.*, 2015) are indicated in bold. *Gps*-coded G3PDH is common in Bacteria and Eukarya but the tree reveals that also quite some archaea possess the *gps* gene. The *gps*-G3PDH homologs found in uncultured MG II/III euryarchaeota genomes are indicated in bold. This tree was constructed using the maximum likelihood method with a WAG model plus gamma distribution and invariant site (WAG+G+I+F). The analysis included 1064 positions in the final dataset. Homologous proteins of the closely related family of the UDP (Uridine diphosphate)-glucose 6-dehydrogenases (UDPG-DH) were used as outgroup to construct the tree. The scale bar represents number of amino acid substitutions per site. Branch support was calculated with the approximate likelihood ratio test (aLRT) and values $\geq 50\%$ are indicated on the branches.

FIGURE 3. Phylogenetic tree of putative archaeal glycerol kinases (*glpK*) and homologous proteins of the xylulose/carbohydrate kinase family. The archaeal *glpK* previously described were grouped in a distinctive cluster, while annotated *glpK* in the ‘Lokiarchaeum’ genome (indicated in bold; Spang *et al.*, 2015) were closely related to carbohydrate kinases of the euryarchaeon *Archaeoglobus fulgidus* and also to xylulose kinases of Bacteria. This tree was constructed using the maximum likelihood method with a LG model plus gamma distribution and invariant site (LG+G+I). The analysis included 585 positions in the final dataset. The scale bar represents number of amino acid substitutions per site. Branch support was calculated with the approximate likelihood ratio test (aLRT) and values $\geq 50\%$ are indicated on the branches.

FIGURE 4. Phylogenetic tree of putative archaeal UgpQ glycerophosphodiester phosphodiesterases (GDPD) and close relatives within the Bacteria. The putative UgpQ GDPDs detected in the ‘Lokiarchaeum’ genome (indicated in bold; Spang *et al.*, 2015) were closely related to a putative UgpQ GDPD in one genome of the DPANN Woesearchaeota, as well as UgpQ detected in bacterial genomes of

the Thermotogae. Homologous proteins of the closely related family of periplasmic GlpQ GDPDs in Bacteria were used as outgroup. This tree was constructed using the maximum likelihood method with a LG model plus gamma distribution and invariant site (LG+G+I). The analysis included 553 positions in the final dataset. The scale bar represents number of amino acid substitutions per site. Branch support was calculated with the approximate likelihood ratio test (aLRT) and values $\geq 50\%$ are indicated on the branches.

FIGURE 5. Bacterial biosynthetic pathway resulting in glycerol diester phospholipids formation.

Fatty acids are synthesized from acyl-ACP via the FAS-II pathway and coupled with G3P to form phospholipids. The hypothetical archaeal fatty acid biosynthetic pathway proposed by Dibrova *et al.* (2014), based on the archaeal acetyl-CoA-acetyltransferase (acetyl-CoA C-acyl transferase; indicated in orange) and bacterial-type enzymes of the β -oxidation of fatty acids (acyl-CoA dehydrogenase, FadE; enoyl-CoA hydratase, FadB1; 3-hydroxyacyl-CoA dehydrogenase, FadB2) operating in reverse direction is indicated in the dashed line box. Enzymes indicated in red have been previously reported to be present as homologs in archaeal genomes, while enzymes in green indicate bacterial enzymes previously concluded to be absent in archaea. Enzymes discussed in the text are indicated with an asterisk. Purple triangles indicate putative homologs in the ‘Lokiarchaeum’ and/or MGII/III genomes (Table 1). Abbreviations: ACP, acyl-carrier protein; MCAT, malonyl-CoA:ACP-transacylase, FabD; KAS, beta-ketoacyl synthase (KAS I, FabB; KAS II, FabF; KAS III, FabH); KR, beta-ketoacyl reductase, FabG; DH, beta-hydroxyacyl dehydratase, FabA/Z; ER, enoyl reductase, FabI; PlsB, glycerol-3-phosphate *O*-acyltransferase; PlsX, acyl-ACP:PO₄ transacylase; PlsY, G3P acyltransferase; PlsC, 1-acylglycerol-3-phosphate *O*-acyltransferase; G3P, glycerol-3-phosphate.

FIGURE 6. Phylogenetic tree of Malonyl-CoA:ACP-transacylase (MCAT, FabD domain), a key enzyme in the pathway of fatty acid synthesis (see Fig. 5 for details). MCAT homologs in archaeal genomes (in bold) and their closest bacterial sequences are shown. This phylogenetic tree was constructed using the maximum likelihood method and the LG model plus gamma distribution and invariant site (LG+G+I). The analysis included 486 positions in the final dataset. The scale bar represents number of amino acid substitutions per site. Branch support was calculated with the approximate likelihood ratio test (aLRT) and values $\geq 50\%$ are indicated on the branches. MGII/III: uncultured marine group II/III euryarchaeota.

FIGURE 7. Phylogenetic tree of the putative archaeal homologs of the PlsY glycerol-3-phosphate acyltransferase and the PlsC 1-acylglycerol-3-phosphate *O*-acyltransferase (see Fig. 5 for details). PlsY and PlsC homologs in archaeal genomes (in bold) and their closest bacterial sequences are shown. This tree was constructed using the maximum likelihood method and the LG model plus gamma distribution and invariant site (LG+G+I). The scale bar represents number of substitutions per site. The analysis included 455 positions in the final dataset. Branch support was calculated with the approximate likelihood ratio test (aLRT) and values $\geq 50\%$ are indicated on the branches. MGII/III: uncultured marine group II/III euryarchaeota.

Supporting information

Fig. S1. Archaeal 16S rRNA gene-based phylogeny modified from Spang *et al.* (2015). TACK, Thaumarchaeota-Aigarchaeota-Crenarchaeota-Korarchaeota superphylum; Bathyarchaeota (Miscellaneous Crenarchaeota Group, MCG and group C3); DSAG, Deep-Sea Archaeal Group/Marine Benthic Group B (including ‘Lokiarchaeum’; Spang *et al.*, 2015); MHVG, Marine Hydrothermal Vent Group; Euryarchaeota superphylum includes the uncultured group II (MGII) and group III (MGIII) euryarchaeota, among others. DPANN superphylum includes Diapherotrites, Parvarchaeota, Aenigmarchaeota, Nanoarchaeota, among others (Castelle *et al.*, 2015).

Fig. S2. Phylogenetic tree of geranylgeranylglyceryl phosphate (GGGP) synthase homologs in archaeal genomes. Tree was constructed using the maximum likelihood method and the LG model plus gamma

distribution and invariant site (LG+G+I). The scale bar represents number of substitutions per site. The analysis included 364 positions in the final dataset. Branch support was calculated with the approximate likelihood ratio test (aLRT) and values $\geq 50\%$ are indicated on the branches. This tree showed the previously reported divergence of GGGP synthases in two different clusters (cluster 1 including the Halobacteriales, Archaeoglobales and Methanomicrobiales, Fig. S2B; and cluster 2 including Thaumarchaeota, Crenarchaeota and GGGP synthases of the rest of euryarchaeotal orders; Fig. S2A; Boucher *et al.*, 2004; Villanueva *et al.*, 2014). The putative GGGP synthase annotated in the 'Lokiarchaeum' genome. This sequence is closely related to GGGP synthases of the Thermoplasmatales, including uncultured marine group II and III euryarchaeota (MGII/III). Fig. S2C indicates the phylogenetic position of the Thaumarchaeota single cell genomes within the tree.

Fig. S3. Phylogenetic tree of putative digeranylgeranyl glyceryl phosphate (DGGGP) synthase homologs in archaeal genomes. This tree is based on the putative archaeal DGGGP synthase phylogenetic tree by Villanueva *et al.* (2014). Tree was constructed using the maximum likelihood method and the LG model plus gamma distribution and invariant site (LG+G+I). The scale bar represents number of amino acid substitutions per site. The analysis included 422 positions in the final dataset. Branch support was calculated with the approximate likelihood ratio test (aLRT) and values $\geq 50\%$ are indicated on the branches. Fig. S3A indicates the phylogenetic relationship between the thaumarchaeotal prenyltransferases and the archaeal DGGGP synthase. Fig. S3B indicates the distribution of the putative DGGGP synthases in the different archaeal groups. The putative DGGGP synthase annotated in the 'Lokiarchaeum' genome (indicated in bold) was closely related to the DGGGP synthases of the euryarchaeotal group Archaeoglobales. Putative DGGGP synthases annotated in the genomes of the uncultured marine group II and III euryarchaeota are not clustered with the rest of the putative DGGGP synthases.

Table S1. Compilation of NCBI accession numbers of the enzymes included in Table 1 for the different archaeal genomes analyzed in this study.

Table S2. Presence (\surd in green) and absence (\times in red) putative homologs of enzymes involved in the archaeal membrane lipid and fatty acid biosynthetic pathways in the 'Lokiarchaeum' genome (Spang *et al.*, 2015) and NCBI accession numbers (see Fig. 1, 5, and text for details).

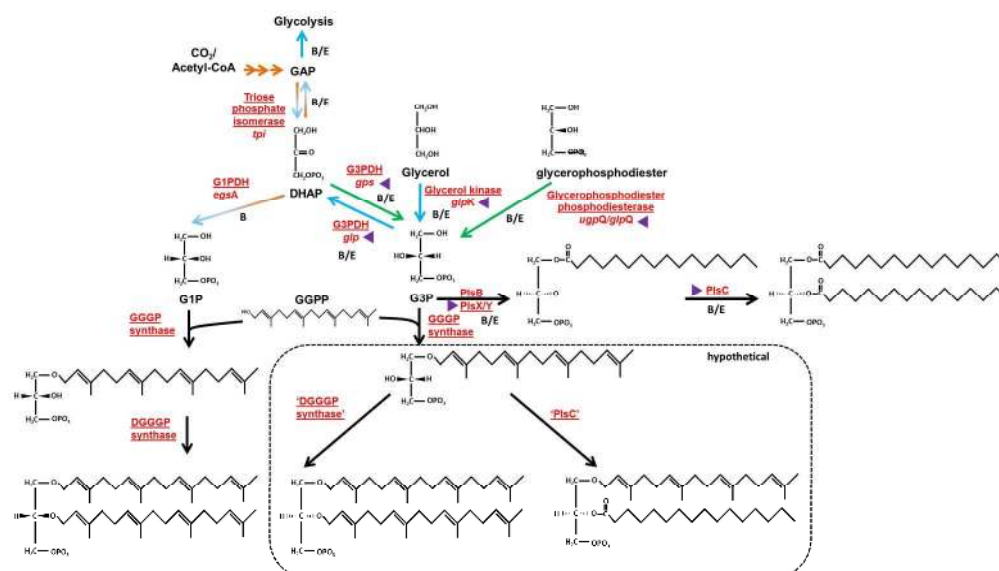


FIGURE 1. Overview of the known and hypothetical diether and ether/ester lipid biosynthetic pathway in Archaea and the related pathway of glycerol metabolism. Autotrophic Archaea produce G1P, which is subsequently incorporated into archaeal membrane lipids, from GAP via DHAP (orange arrows). The glycerol metabolism pathway of heterotrophic Archaea, which feeds glycerol into the glycolysis pathway, is indicated with blue arrows. The green arrows indicate the here-proposed formation of G3P from DHAP by *gps*-coded G3PDH, commonly only found in Bacteria and Eukarya, and the formation of G3P from the degradation of glycerophosphodiesters by a glycerophosphodiester phosphodiesterase (GDPD) (see text for details). Some other reactions are also performed by these organisms as indicated (B= Bacteria; E= Eukarya). Arrows in gradient orange/blue indicate steps performed by both auto- and heterotrophic archaea. Purple triangles indicate putative homologs in the 'Lokiarchaeum' and/or MGII/III genomes (Table 1). Steps included in the dashed line box are hypothetical and based on the predicted occurrence of specific enzymes (Table 1; Table S1) as discussed in the text. The names of enzymes are underlined and in case where the genes encoding for these enzymes have specific names they are given in italics. Abbreviations used: GAP, d-Glyceraldehyde-3-phosphate; G1P, Glycerol-1-phosphate; G3P, Glycerol-3-phosphate; GGGP, geranylgeranylgeranyl phosphate; DGGGP, digeranylgeranylgeranyl phosphate; DHAP, Dihydroxyacetone phosphate; G1PDH, glycerol-1-phosphate dehydrogenase; G3PDH, glycerol-3-phosphate dehydrogenase. "?" indicates an hypothetical enzyme similar to GGGP synthase but with a G3P stereo-chemistry as indicate din the text. 'DGGGP synthase' and 'PlsC' indicate hypothetical enzymes that are expected to perform a similar reaction to the original ones.

470x267mm (150 x 150 DPI)

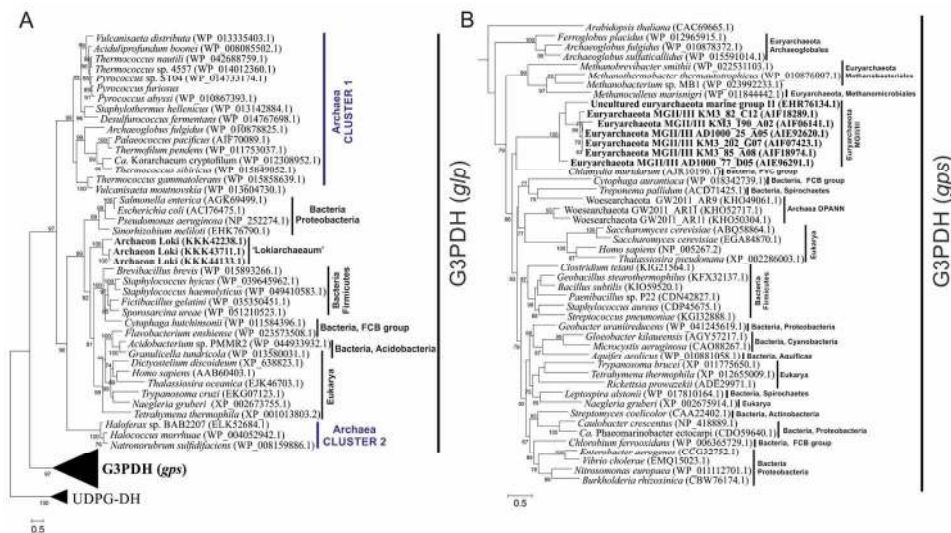


FIGURE 2. Phylogenetic tree of sn-glycerol-3-phosphate dehydrogenases (G3PDH). The tree clearly reveals two main clusters of G3PDH encoded by the *glp* (A) and *gps* (B) genes. These different forms of G3PDH catalyze the conversion of G3P into DHAP and the reverse reaction, respectively (see Fig. 1). *Glp*-coded G3PDH is common in Bacteria, Eukarya and Archaea, where it is one of the enzymes involved in feeding glycerol into the glycolysis pathway. The putative *glp*-G3PDH homologs found in the composite 'Lokiarchaeum' genome (Spang et al., 2015) are indicated in bold. *Gps*-coded G3PDH is common in Bacteria and Eukarya but the tree reveals that also quite some archaea possess the *gps* gene. The *gps*-G3PDH homologs found in uncultured MG II/III euryarchaeota genomes are indicated in bold. This tree was constructed using the maximum likelihood method with a WAG model plus gamma distribution and invariant site (WAG+G+I+F). The analysis included 1064 positions in the final dataset. Homologous proteins of the closely related family of the UDP (Uridine diphosphate)-glucose 6-dehydrogenases (UDPG-DH) were used as outgroup to construct the tree. The scale bar represents number of amino acid substitutions per site. Branch support was calculated with the approximate likelihood ratio test (aLRT) and values $\geq 50\%$ are indicated on the branches.

306x172mm (150 x 150 DPI)

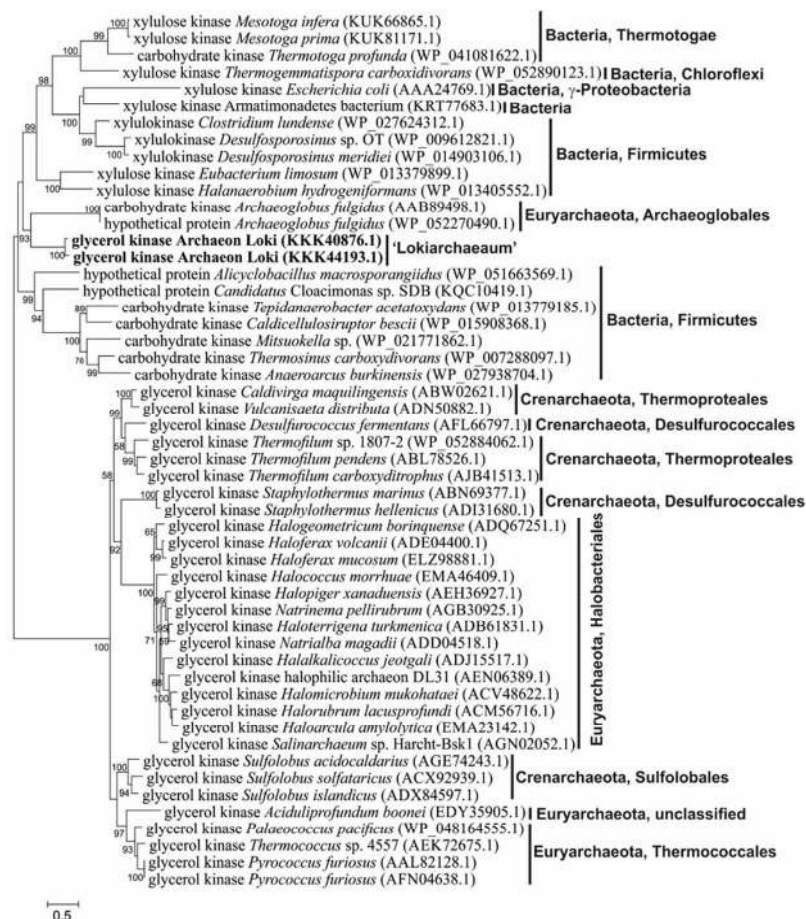


FIGURE 3. Phylogenetic tree of putative archaeal glycerol kinases (glpK) and homologous proteins of the xylulose/carbohydrate kinase family. The archaeal glpK previously described were grouped in a distinctive cluster, while annotated glpK in the 'Lokiarchaeum' genome (Spang et al., 2015; indicated in bold) were closely related to carbohydrate kinases of the euryarchaeon *Archaeoglobus fulgidus* and also to xylulose kinases of Bacteria. This tree was constructed using the maximum likelihood method with a LG model plus gamma distribution and invariant site (LG+G+I). The analysis included 585 positions in the final dataset. The scale bar represents number of amino acid substitutions per site. Branch support was calculated with the approximate likelihood ratio test (aLRT) and values $\geq 50\%$ are indicated on the branches.

198x184mm (150 x 150 DPI)

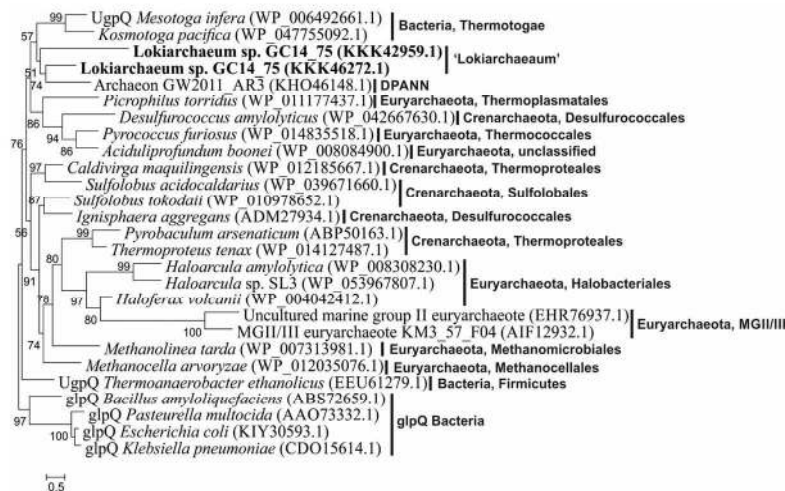


FIGURE 4. Phylogenetic tree of putative archaeal UgpQ glycerophosphodiester phosphodiesterases (GDPD) and close relatives within the Bacteria. The putative UgpQ GDPDs detected in the 'Lokiarchaeum' genome (Spang et al., 2015; indicated in bold) were closely related to a putative UgpQ GDPD in one genome of the DPANN Woese archaeota, as well as UgpQ detected in bacterial genomes of the Thermotogae. Homologous proteins of the closely related family of periplasmic GlpQ GDPDs in Bacteria were used as outgroup. This tree was constructed using the maximum likelihood method with a LG model plus gamma distribution and invariant site (LG+G+I). The analysis included 553 positions in the final dataset. The scale bar represents number of amino acid substitutions per site. Branch support was calculated with the approximate likelihood ratio test (aLRT) and values $\geq 50\%$ are indicated on the branches.

301x153mm (150 x 150 DPI)

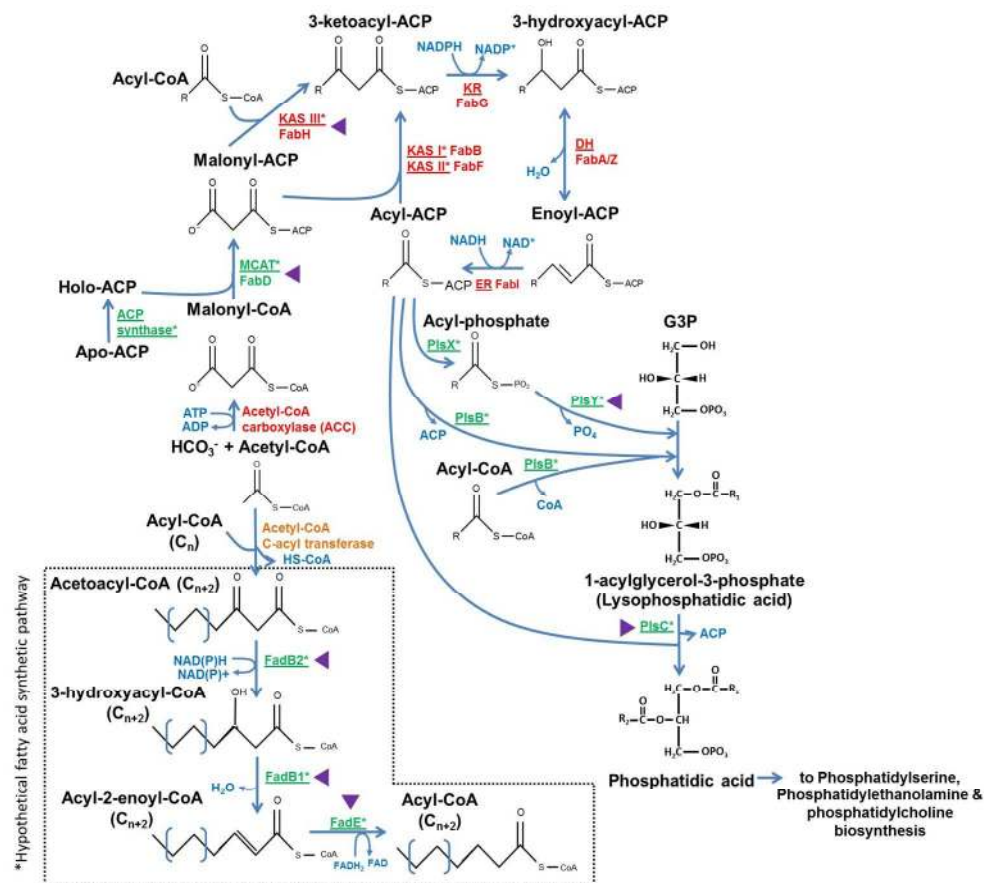


FIGURE 5. Bacterial biosynthetic pathway resulting in glycerol diester phospholipids formation. Fatty acids are synthesized from acyl-ACP via the FAS-II pathway and coupled with G3P to form phospholipids. The hypothetical archaeal fatty acid biosynthetic pathway proposed by Dibrova et al. (2014), based on the archaeal acetyl-CoA-acetyltransferase (acetyl-CoA C-acyl transferase; indicated in orange) and bacterial-type enzymes of the β -oxidation of fatty acids (acyl-CoA dehydrogenase, FadE; enoyl-CoA hydratase, FadB1; 3-hydroxyacyl-CoA dehydrogenase, FadB2) operating in reverse direction is indicated in the dashed line box. Enzymes indicated in red have been previously reported to be present as homologs in archaeal genomes, while enzymes in green indicate bacterial enzymes previously concluded to be absent in archaea. Enzymes discussed in the text are indicated with an asterisk. Purple triangles indicate putative homologs in the 'Lokiarchaeum' and/or MGII/III genomes (Table 1). Abbreviations: ACP, acyl-carrier protein; MCAT, malonyl-CoA:ACP-transacylase, FabD; KAS, beta-ketoacyl synthase (KAS I FabB; KAS II, FabF; KAS III, FabH); KR, beta-ketoacyl reductase, FabG; DH, beta-hydroxyacyl dehydratase, FabA/Z; ER, enoyl reductase, FabI; PlsB, glycerol-3-phosphate O-acyltransferase; PlsX, acyl-ACP:PO₄ transacylase; PlsY, G3P acyltransferase; PlsC, 1-acylglycerol-3-phosphate O-acyltransferase; G3P, glycerol-3-phosphate.

327x288mm (150 x 150 DPI)

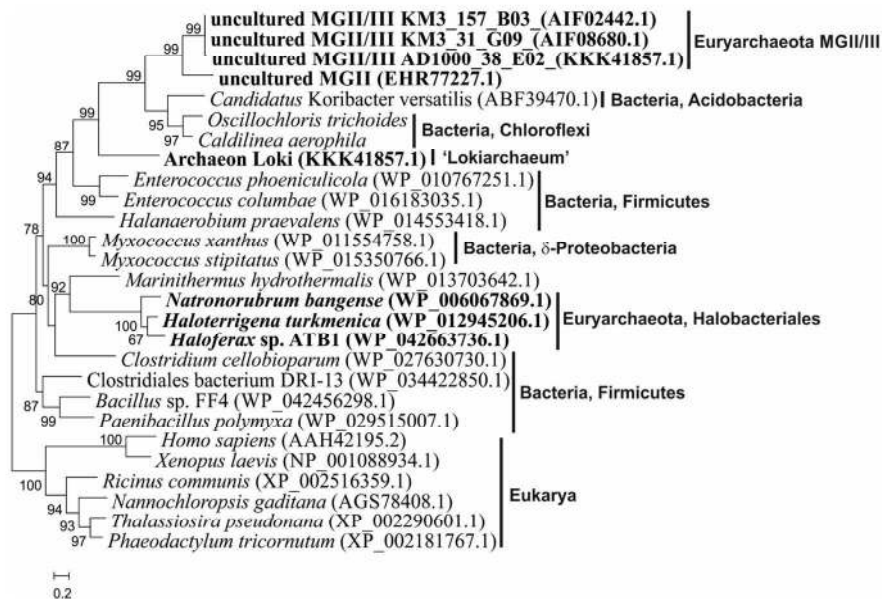


FIGURE 6. Phylogenetic tree of Malonyl-CoA:ACP-transacylase (MCAT, FabD domain), a key enzyme in the pathway of fatty acid synthesis (see Fig. 5 for details). MCAT homologs in archaeal genomes (in bold) and their closest bacterial sequences are shown. This phylogenetic tree was constructed using the maximum likelihood method and the LG model plus gamma distribution and invariant site (LG+G+I). The analysis included 486 positions in the final dataset. The scale bar represents number of amino acid substitutions per site. Branch support was calculated with the approximate likelihood ratio test (aLRT) and values $\geq 50\%$ are indicated on the branches. MGII/III: uncultured marine group II/III euryarchaeota.

267x173mm (150 x 150 DPI)

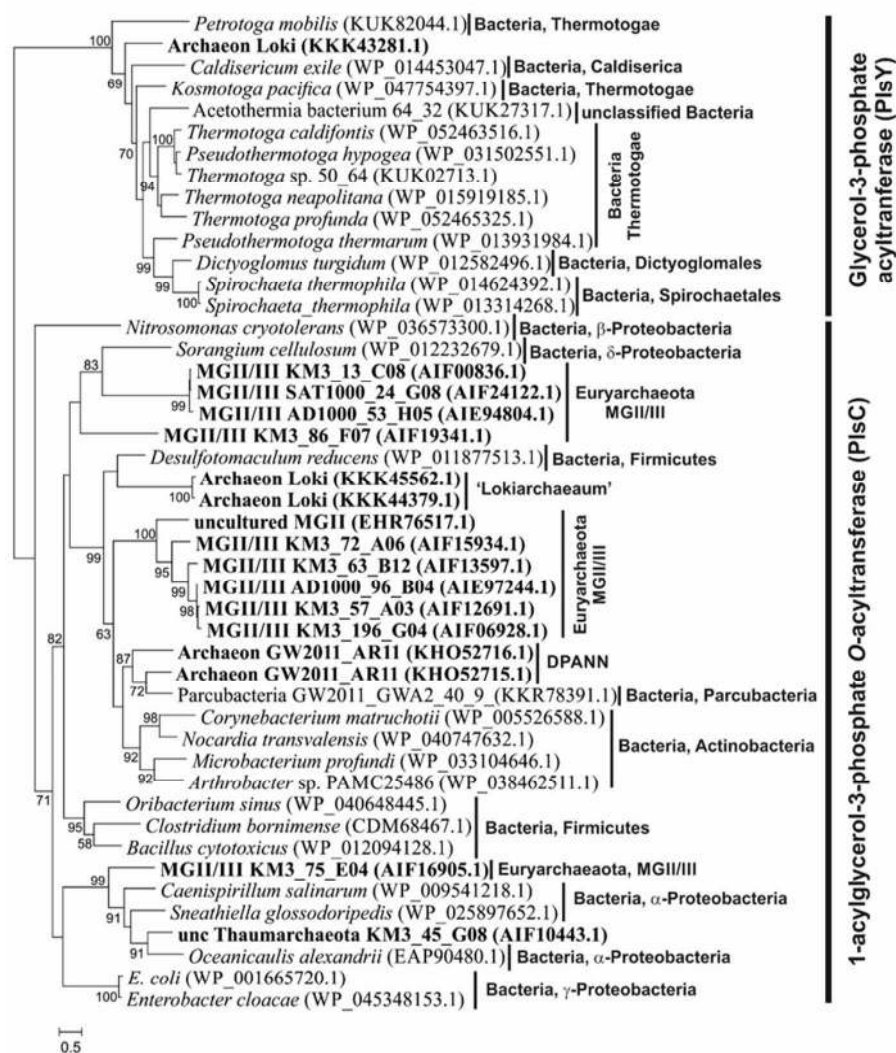


FIGURE 7. Phylogenetic tree of the putative archaeal homologs of the PlsY glycerol-3-phosphate acyltransferase and the PlsC 1-acylglycerol-3-phosphate O-acyltransferase (see Fig. 5 for details). PlsY and PlsC homologs in archaeal genomes (in bold) and their closest bacterial sequences are shown. This tree was constructed using the maximum likelihood method and the LG model plus gamma distribution and invariant site (LG+G+I). The scale bar represents number of substitutions per site. The analysis included 455 positions in the final dataset. Branch support was calculated with the approximate likelihood ratio test (aLRT) and values $\geq 50\%$ are indicated on the branches. MGII/III: uncultured marine group II/III euryarchaeota.

170x186mm (150 x 150 DPI)

Figure 1

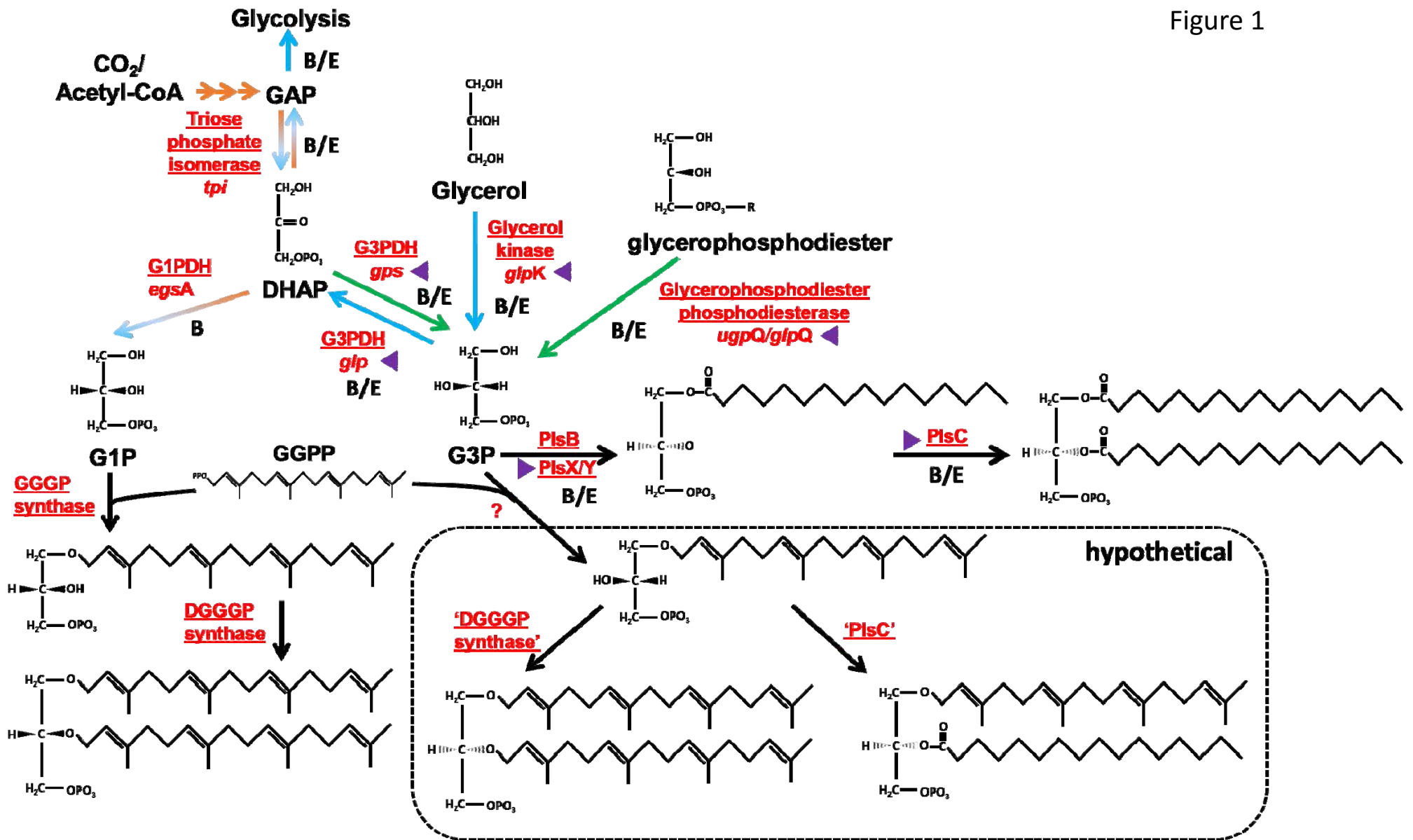


Figure 2

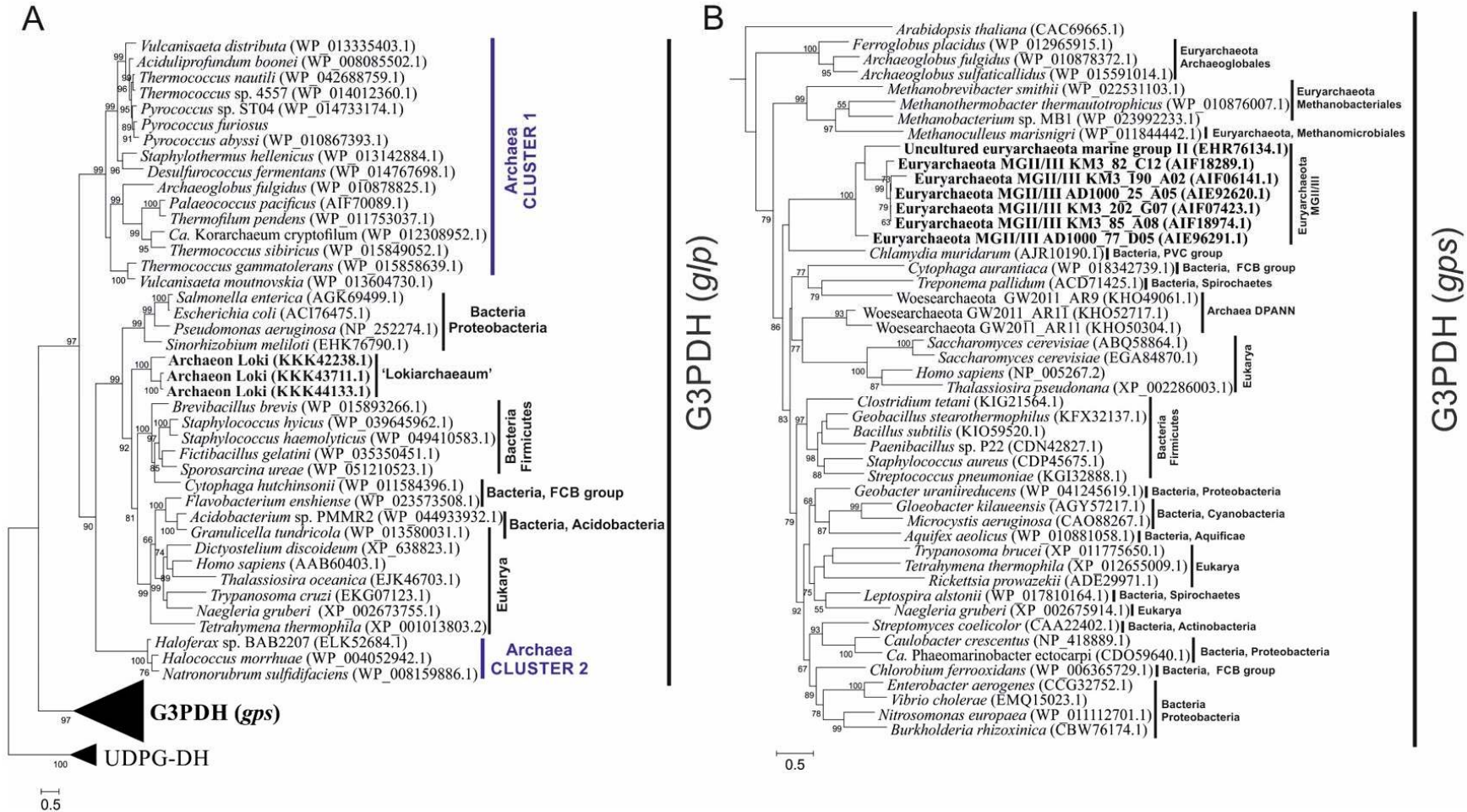


Figure 3

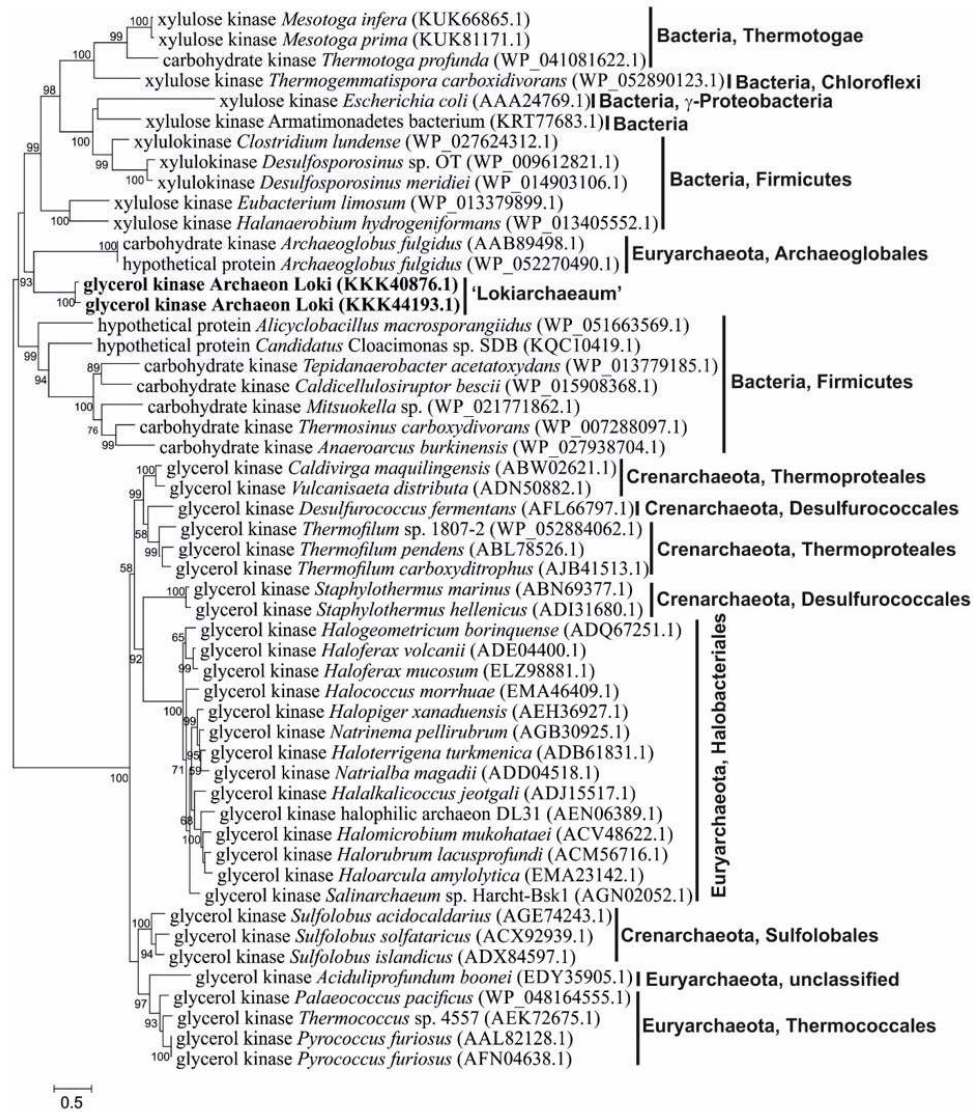


Figure 4

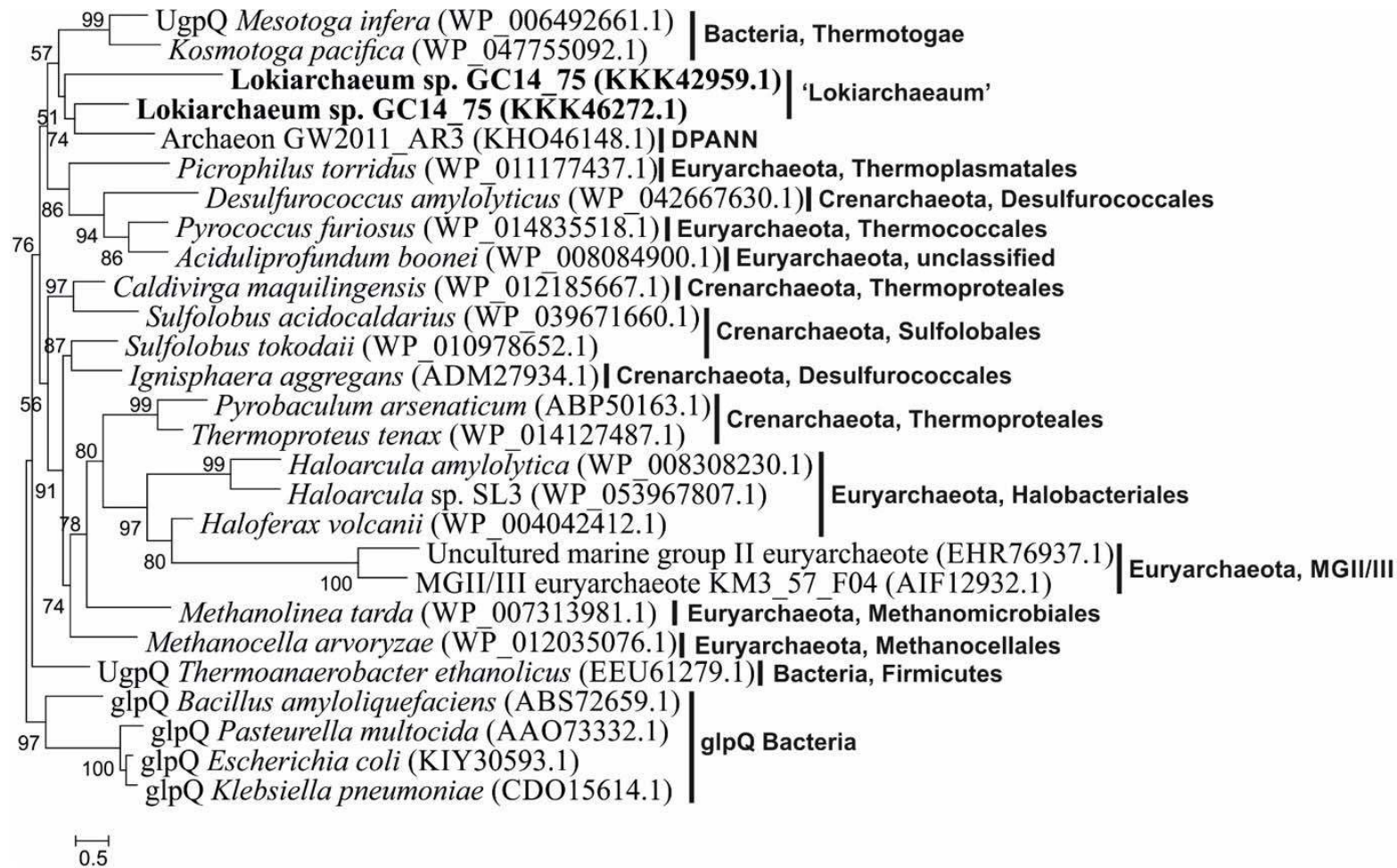


Figure 5

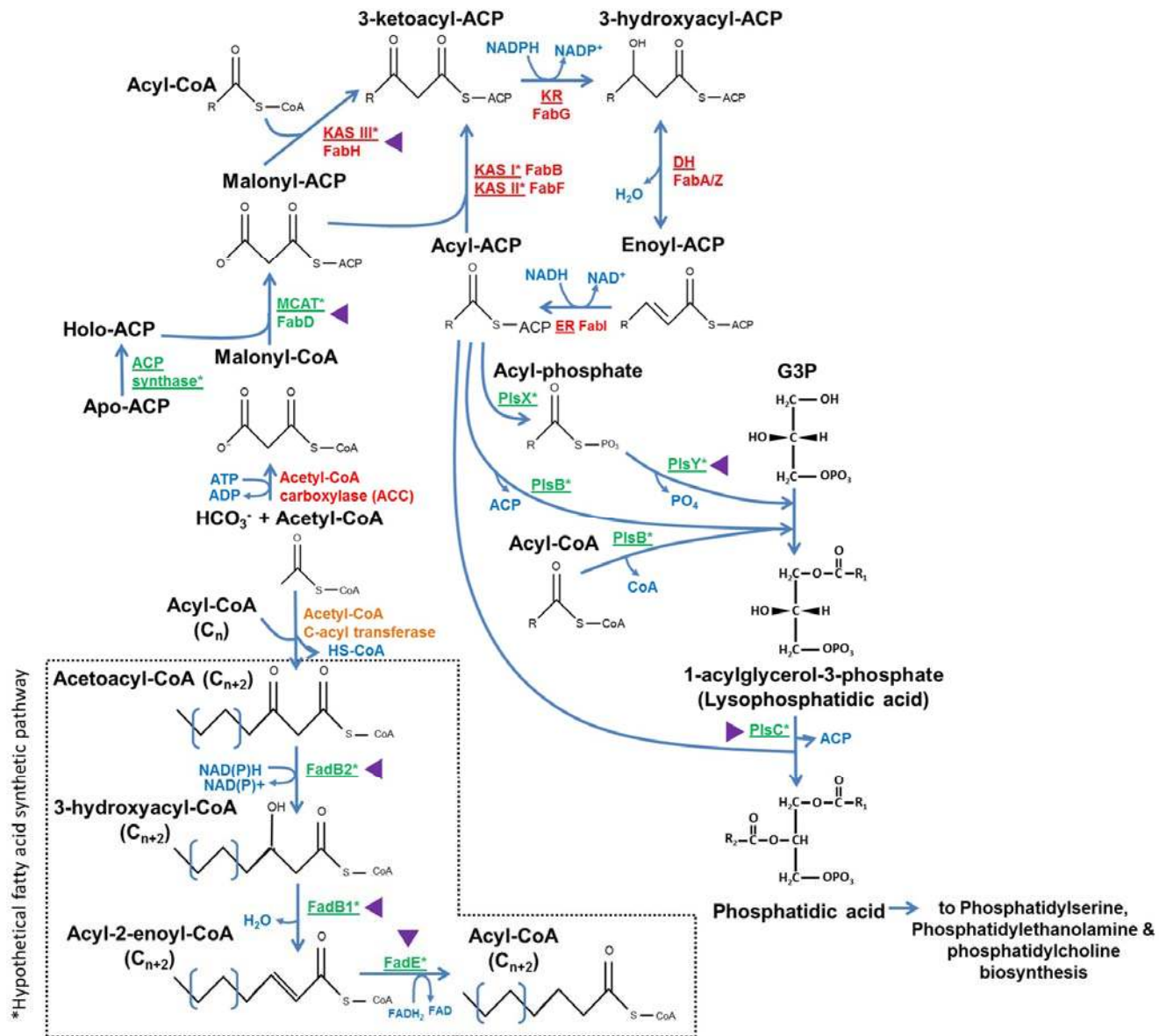
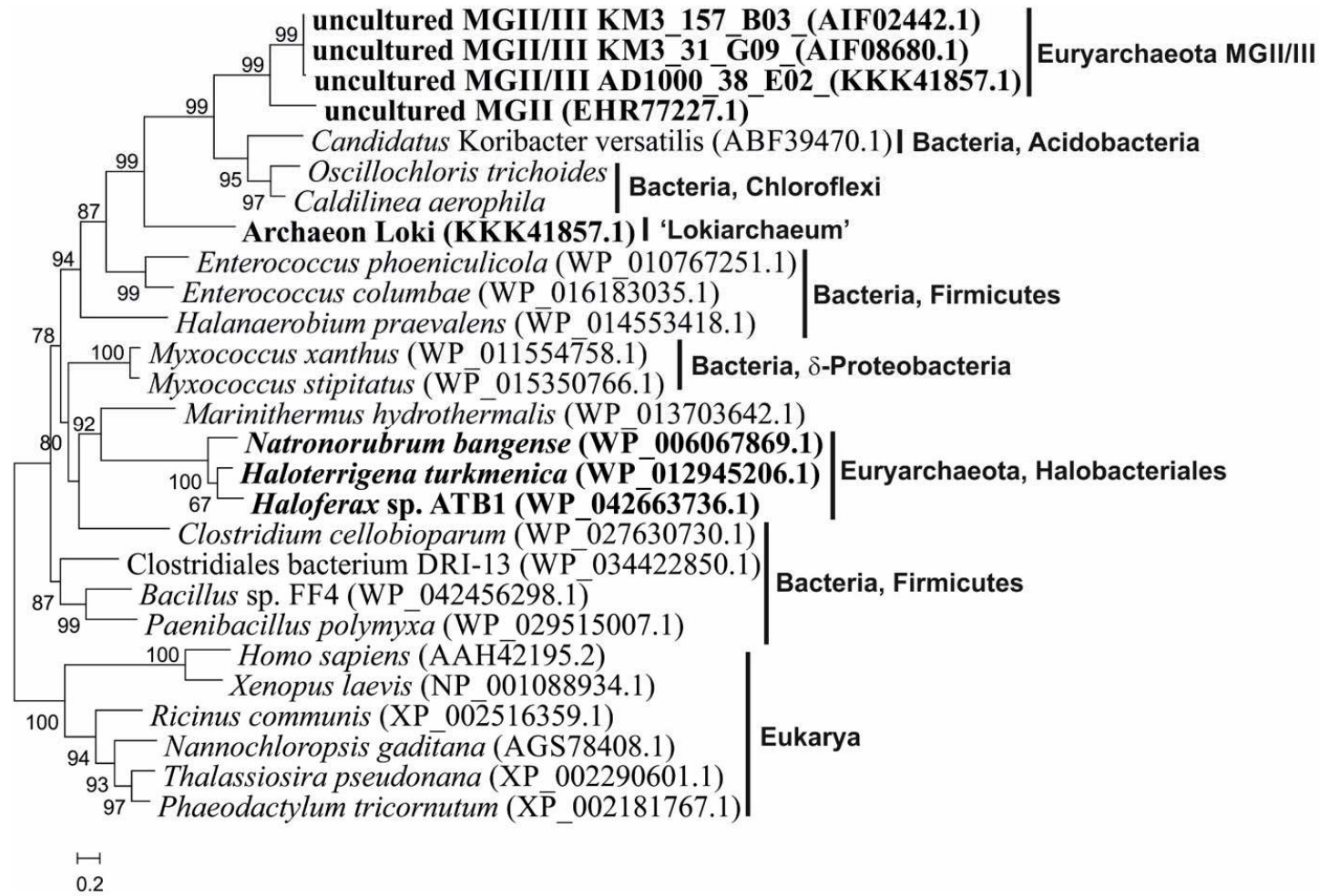


Figure 6



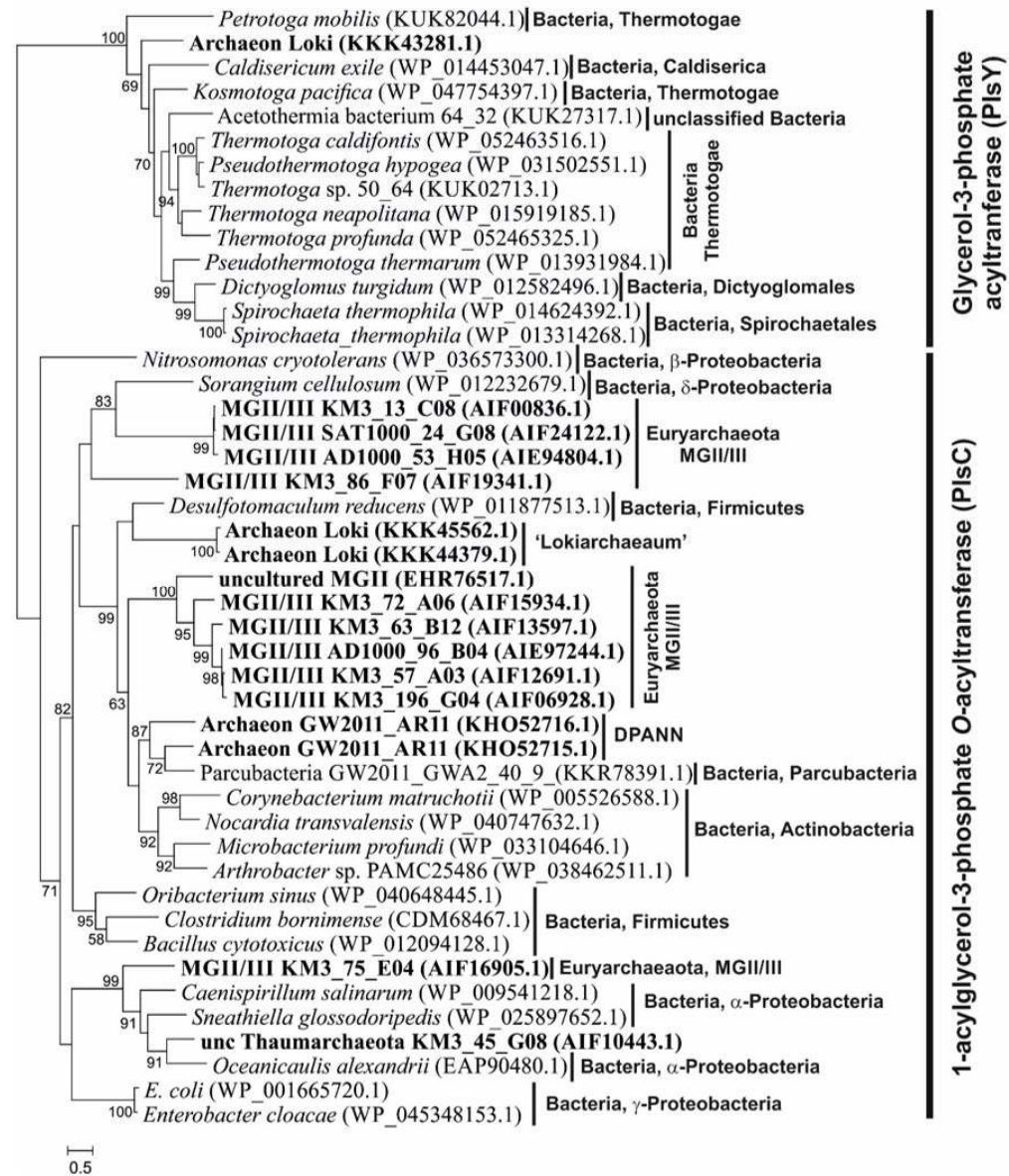
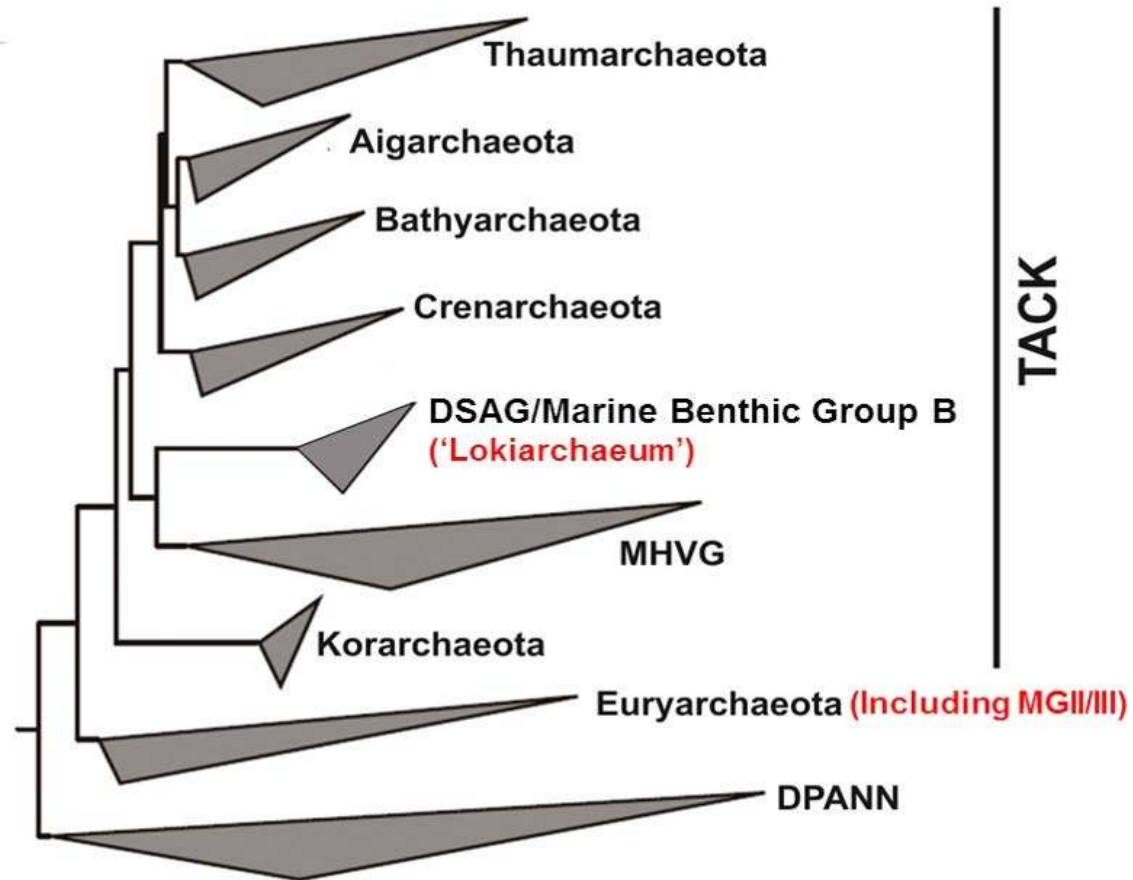


Figure 7

Figure S1



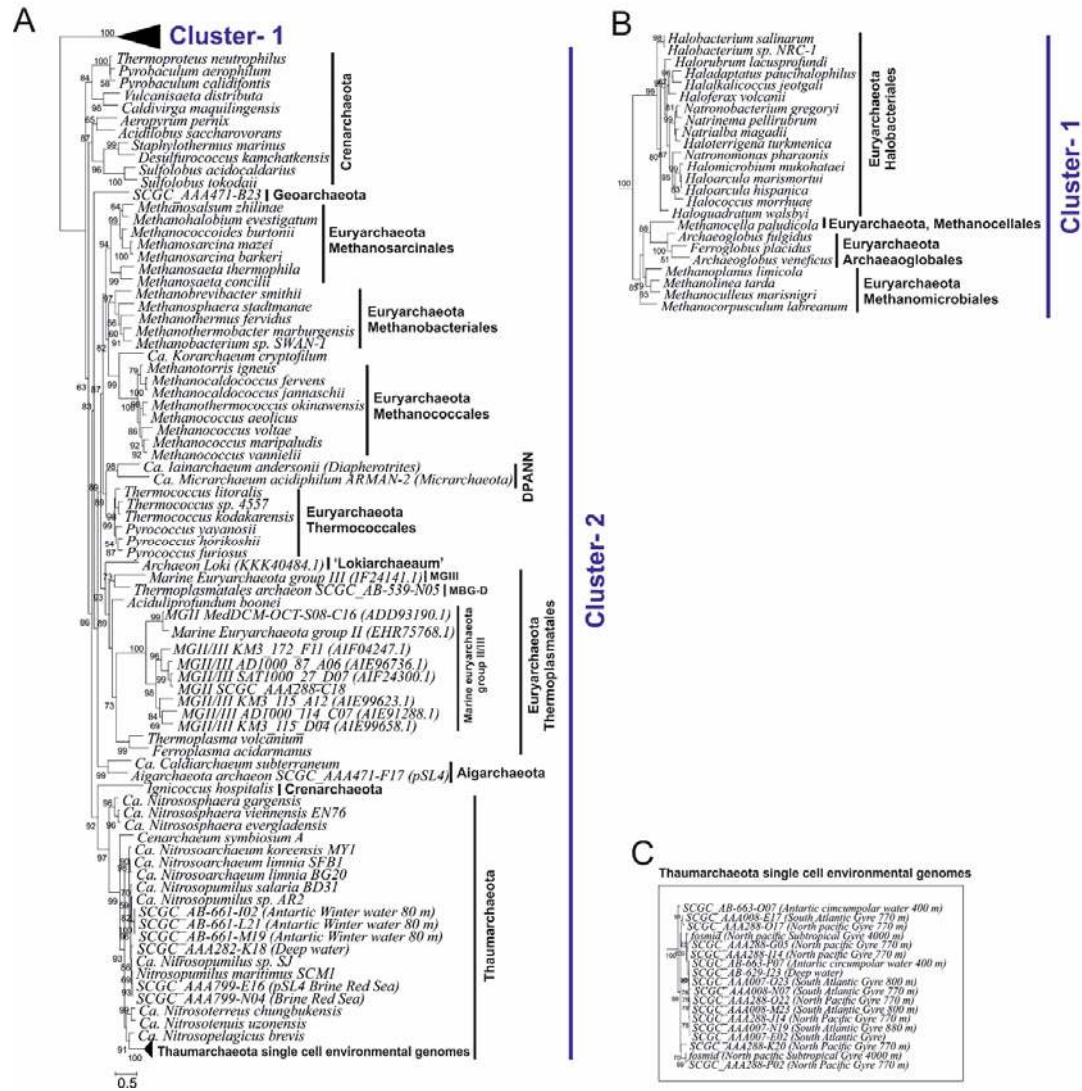
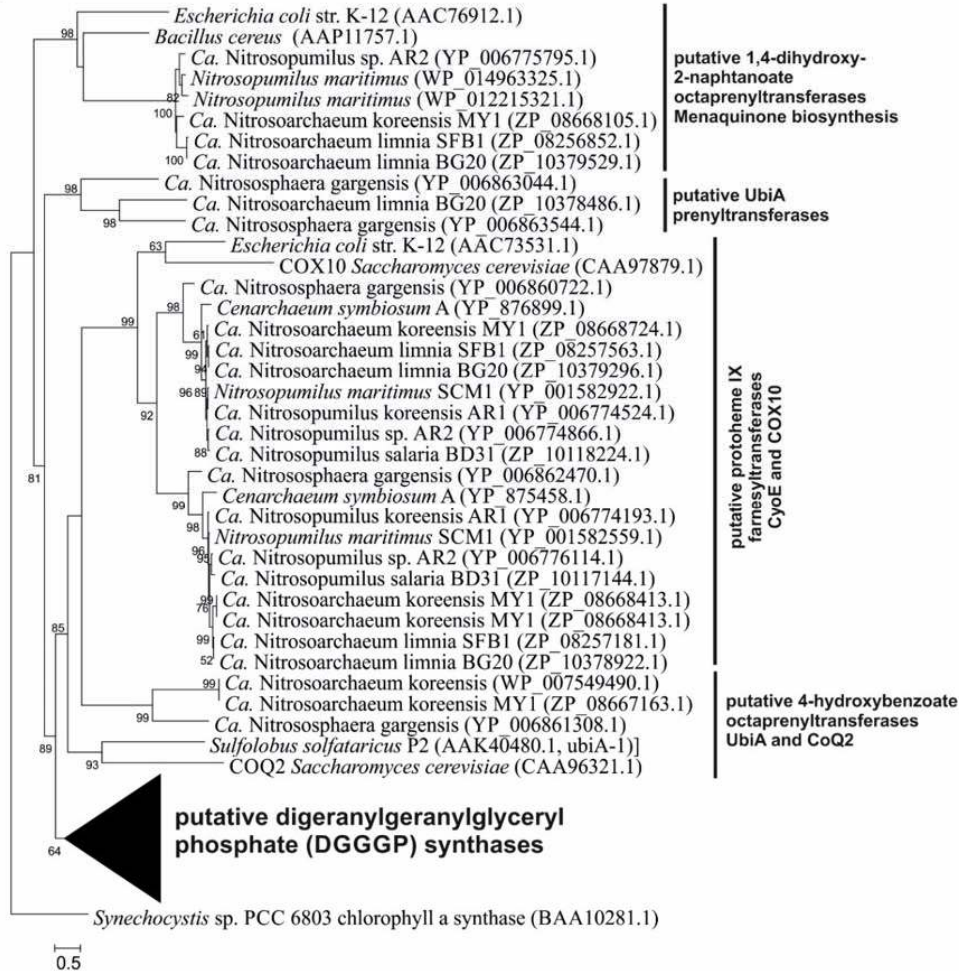


Figure S2

Figure S3

A



B

